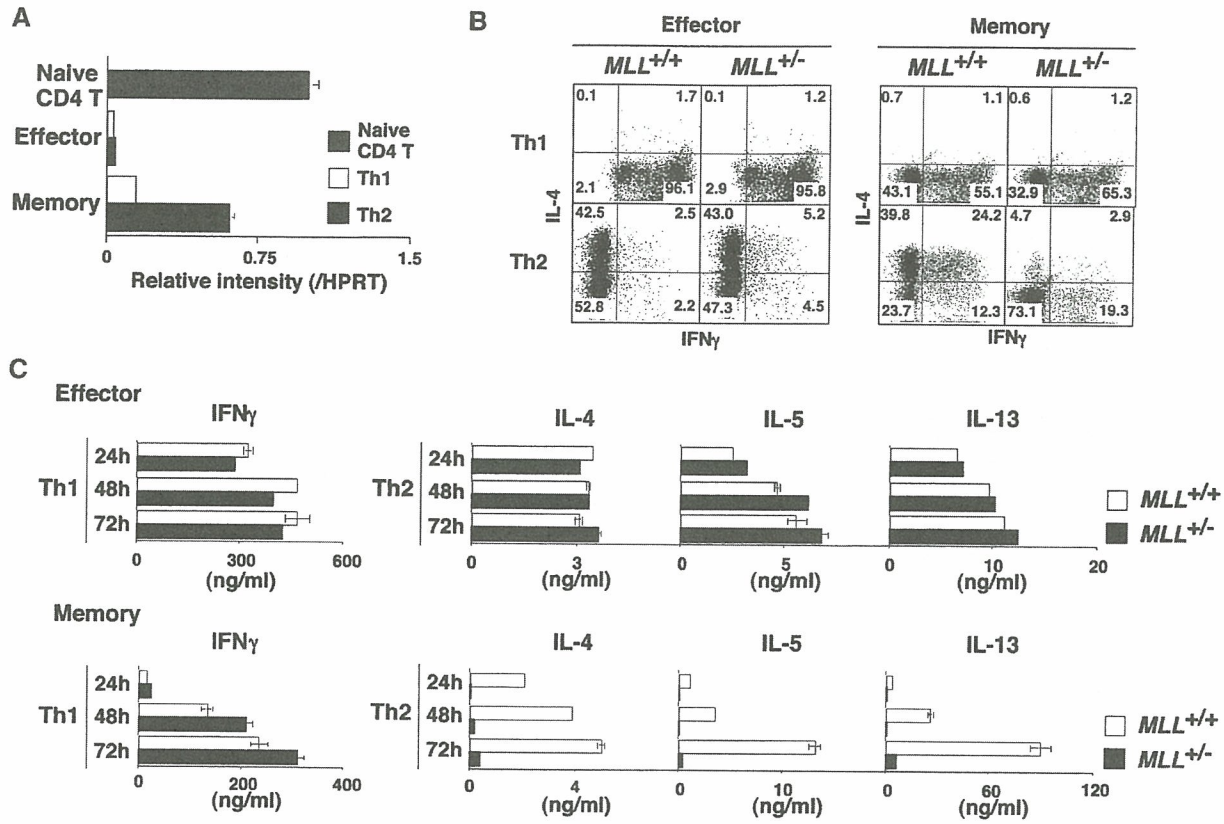

Figure 1. The Ability to Produce Th2 Cytokines in *MLL*$^{+/-}$ Effector and Memory Th2 Cells

(A) MLL mRNA expression in naive CD4 T, and effector and memory Th1/Th2 cells. The expression levels of MLL and HPRT mRNA were determined by quantitative RT-PCR. Relative intensity (mean of three samples) with standard deviation is shown.

(B) Decreased IL-4-producing cells in *MLL*$^{+/-}$ memory Th2 cells. Intracellular staining profiles of IFNγ and IL-4, after stimulation with PMA (10 ng/ml) plus Ionomycin (500 nM) for 4 hr, are shown with the percentages of cells in each area. Three independent experiments were done with similar results.

(C) Decreased Th2 cytokine production in *MLL*$^{+/-}$ memory Th2 cells. Effector and memory Th1/Th2 cells were stimulated in vitro with OVA plus APC for the indicated hours, and the concentration of cytokines (IL-4, IL-5, IL-13, and IFNγ) in the culture supernatant was determined by ELISA. The mean values of triplicate cultures with standard deviations are shown. Five independent experiments were performed with similar results.

effector Th2 cells were purified by an affinity matrix technique and flow cytometry (Figure 3A, top). The Th2 cells were subjected to resting culture conditions as described in the Experimental Procedures, and then the ability to produce Th2 cytokines was assessed after restimulation with immobilized anti-TCR mAb. In *MLL*$^{+/-}$ Th2 cells as compared to *MLL*$^{+/+}$ Th2 cells, the number of IL-4-producing cells (78.9% versus 49.3%) and the values of MFI for IL-4 staining (130 versus 52) were significantly reduced (Figure 3A, bottom). The ability to produce Th2 cytokines (IL-4, IL-5, and IL-13) was decreased significantly in *MLL*$^{+/-}$ Th2 cells (Figure 3B). The levels of histone H3-K4 methylation at the Th2 cytokine gene loci (CGRE, CNS1, V_A enhancer, CNS2, IL-4p, IL-13p, and IL-5p) assessed by a quantitative PCR analysis were significantly decreased, whereas those at RAD50 promoter and IFNγ promoter were equivalent (Figure 3C). Moreover, we tested the protein expression levels of various transcription factors that are important for Th2 cytokine production and Th2 cell differentiation. The expression of GATA3 protein was substantially decreased in *MLL*$^{+/-}$ Th2 cells, while the levels of c-Maf, JunB, NFAT1, and NFAT2 proteins were equivalent (Figure 3D). These results indicate that *MLL*$^{+/-}$ effector Th2 cells fail to maintain properly the ability to produce Th2 cytokines and the histone modification under resting culture conditions in vitro.

MLL$^{+/-}$ Memory Th2 Cells Fail to Maintain GATA3 Expression

The expression levels of GATA3, NFAT1, NFAT2, JunB, and c-Maf in the in vitro generated effector Th2 cells and freshly prepared memory Th2 cells were assessed. The levels of GATA3 mRNA appeared to be normal in *MLL*$^{+/-}$ effector Th2 cells, but those in *MLL*$^{+/-}$ memory Th2 cells were substantially decreased (Figure 4A). However, no significant effect was observed in the expression of NFAT1, NFAT2, JunB, c-Maf, p300, or CBP in either the *MLL*$^{+/-}$ effector or memory Th2 cells. mRNA levels of Meis, one of the authentic MLL target genes, were decreased to about a half in *MLL*$^{+/-}$ memory Th2 cells as compared to those in *MLL*$^{+/+}$ memory cells. The expression of other known MLL target genes, including Hoxa7, Hoxc8, and Hoxa9, was not detected in either effector or memory Th2 cells (data not shown). The protein expression levels of GATA3 also selectively decreased in the *MLL*$^{+/-}$ memory Th2 cells but not *MLL*$^{+/-}$ effector Th2 cells (Figure S4). In addition, the

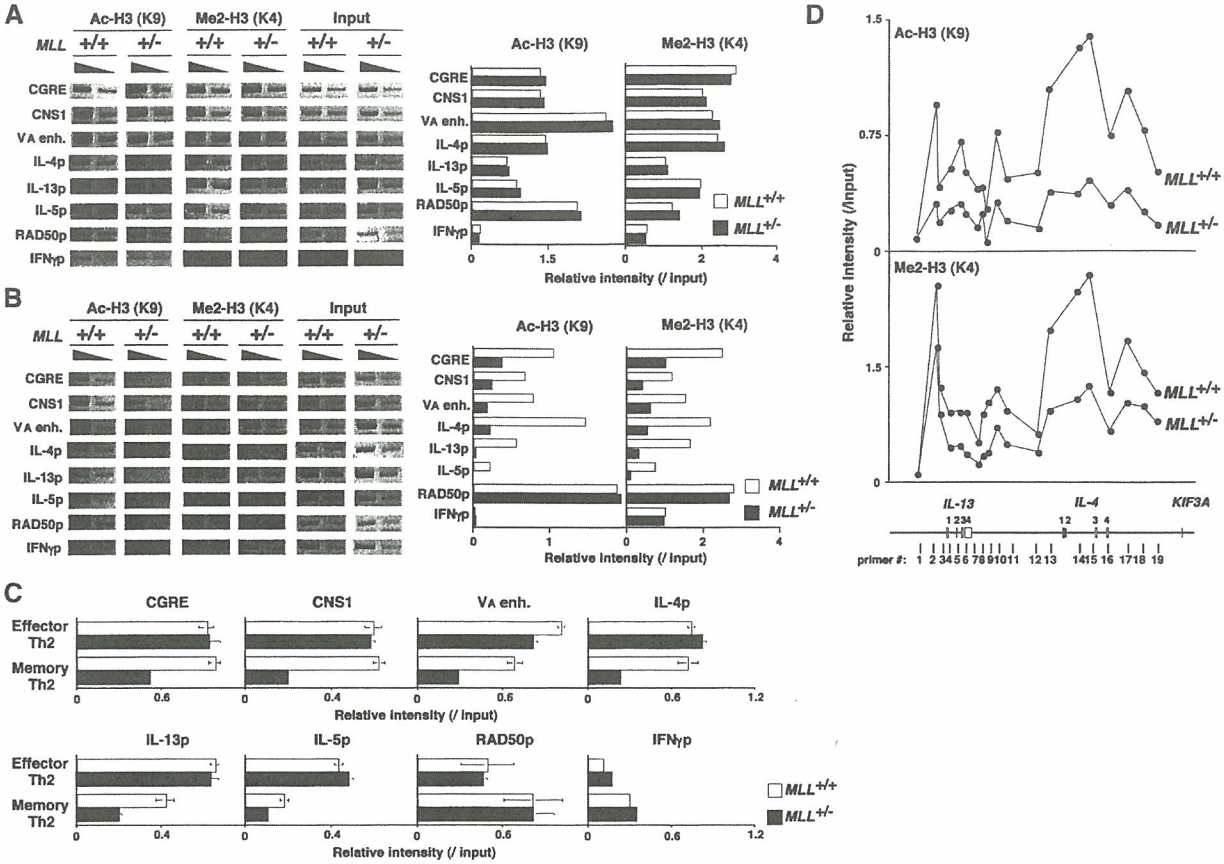

Figure 2. Acetylation of Histone H3-K9 and Methylation of H3-K4 at the Th2 Cytokine Gene Loci in $MLL^{+/-}$ Effector and Memory Th2 Cells

Effector Th2 cells (A) and memory Th2 cells (B) were generated from $MLL^{+/-}$ mice. A ChIP assay was performed with anti-acetylhistone H3-K9 and anti-dimethylhistone H3-K4 antibodies and indicated specific primer pairs. Three regulatory elements (CGRE, 1.6 Kb upstream of IL-13 exon1 [Yamashita et al., 2002]; CNS1, intergenic region between IL-13 and IL-4 [Loots et al., 2000]; and V_A enhancer region, downstream of IL-4 gene [Agarwal et al., 2000]) were included.

(A and B) PCR was performed with a 3-fold serial dilution of template genomic DNA. Three independent experiments in each panel were performed with similar results. The relative band intensities (/input) are shown.

(C) The levels of histone H3-K4 methylation were determined by quantitative PCR. The relative intensity (/input) (mean of three samples) is shown with standard deviations.

(D) A representative result of a ChIP analysis with a series of primer pairs covering the IL-4/IL-13 gene loci. Shown is the relative intensity (/input) of each primer pair. The PCR product bands are shown in Figure S3. Three independent experiments in each panel were performed with similar results.

overexpression of GATA3 into $MLL^{+/-}$ memory Th2 cells partially but significantly restored the generation of IL-4-producing Th2 cells (Figure S5), suggesting that the decrease in Th2 cytokine production in $MLL^{+/-}$ memory Th2 cells is due at least in part to a decreased expression of GATA3 in $MLL^{+/-}$ memory Th2 cells.

Thus, we next assessed the histone modifications of the GATA3 gene locus and found the levels of histone H3-K9 acetylation and H3-K4 methylation at the promoter (GATA3p) and intron 1 (GATA3 int1) region to be significantly decreased in the $MLL^{+/-}$ memory Th2 cells (Figure 4B). No decrease was detected in the $MLL^{+/-}$ effector Th2 cells. To further investigate the chromatin status of the GATA3 gene locus, a series of primer pairs covering the GATA3 locus was prepared and used in a ChIP assay. Although the decrease in the levels of histone H3-K9 acetylation was modest, the levels of histone H3-K4 methylation from the 5 Kb upstream of exon 1 through the end of exon 5 were substantially decreased in the $MLL^{+/-}$ memory Th2 cells (Figure 4C and Figure S6). The methylation levels of H3-K4 of selected regions in the GATA3 locus were also determined by ChIP assay with quantitative PCR. We designated an upstream conserved noncoding sequence (~2.5–3.0 Kb upstream of the GATA3 exon1) as GATA3-CNS1 and included this for the analysis. A significant reduction in histone H3-K4 methylation at GATA3-CNS1, GATA3 promoter (GATA3p), GATA3 exon2, and GATA3 intron2 was confirmed in the $MLL^{+/-}$ memory Th2 cells (Figure 4D). These results suggest that the chromatin status of the GATA3 gene locus is relatively closed in $MLL^{+/-}$ memory Th2 cells in comparison to $MLL^{+/+}$ memory Th2 cells.

The Expression of MLL Controls the Maintenance of Histone Modifications of the GATA3 Locus and the Th2 Cytokine Gene Loci in Established Th2 Cell Lines

Next, in order to assess whether the expression level of MLL controls the maintenance of histone modifications at the GATA3 gene locus and the Th2 cytokine gene

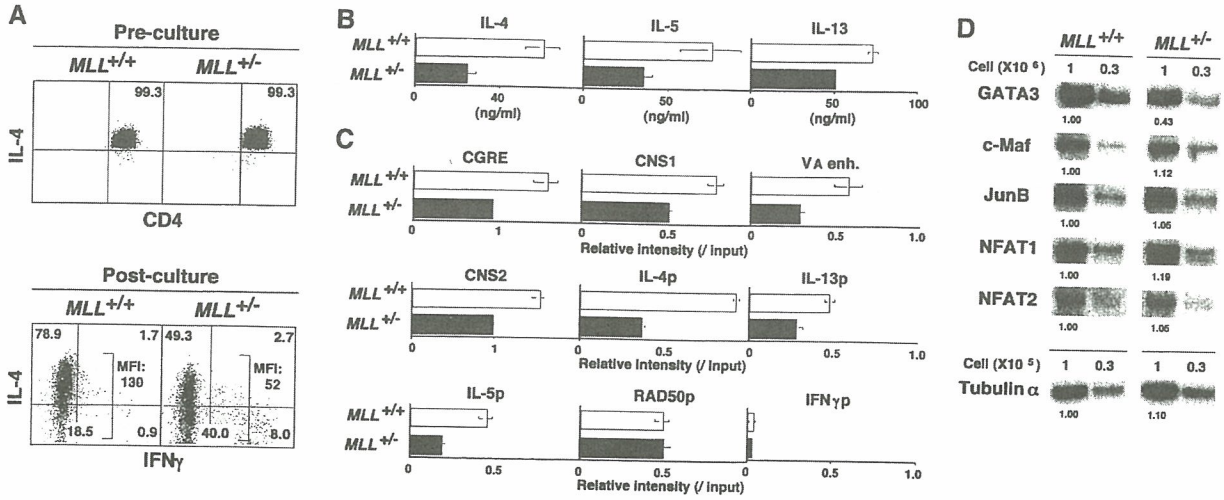

Figure 3. *MLL*$^{+/-}$ Effector Th2 Cells Fail to Maintain Th2 Cytokine Production and Histone H3-K4 Methylation In Vitro

(A) Decreased IL-4-production in *MLL*$^{+/-}$ effector Th2 cells maintained under resting culture conditions in vitro. Three independent experiments were done with similar results.

(B) *MLL*$^{+/-}$ Th2 cells maintained under resting culture conditions were stimulated with immobilized anti-TCR mAb for 16 hr, and the production of indicated cytokines was determined by ELISA. The mean values of triplicate cultures with standard deviations are shown. Three independent experiments were performed with similar results.

(C) The levels of histone H3-K4 methylation at Th2 cytokine gene loci in *MLL*$^{+/+}$ and *MLL*$^{+/-}$ Th2 cells maintained under resting culture conditions were determined by a ChIP assay with a quantitative PCR analysis as described in Figure 2C. The relative intensity (/input) (mean of three samples) is shown with standard deviations.

(D) The protein expression of GATA3, c-Maf, JunB, NFAT1, and NFAT2 in *MLL*$^{+/-}$ Th2 cells maintained under resting culture conditions. Immunoblotting with specific mAbs was performed. Band intensities were measured with a densitometer, and arbitrary densitometric units are shown.

loci, several stable MLL knockdown Th2 (D10G4.1) cell lines were established by means of a siRNA vector for MLL. As expected, the MLL knockdown cells (MLL KD#1, #2, and #3) showed decreased MLL mRNA to varying degrees, and a corresponding reduction of GATA3 mRNA was observed in parallel for each line (Figure 5A). In contrast, the expression levels of c-Maf, JunB, CBP, and p300 mRNA were unaffected (data not shown). The expression of IL-4, IL-5, and IL-13 mRNA upon PMA+Ionomycin stimulation was significantly decreased after the introduction of siRNA for MLL (Figure 5B). Similar results were obtained via a MLL siRNA vector targeted to a different site (data not shown).

Next, we assessed further the histone modifications at the GATA3 locus and the Th2 cytokine gene loci in MLL knockdown cells. The levels of histone H3-K9 acetylation and H3-K4 methylation at the GATA3 gene locus decreased after the introduction of siRNA for MLL (Figure 5C). Similarly, the levels of both histone modifications at the Th2 cytokine gene loci (CGRE, CNS1, V_A enhancer, IL-4 promoter, IL-13 promoter, and IL-5 promoter) were decreased in MLL knockdown cell lines, and representative results in MLL KD#1 are shown in Figure 5D. Histone modifications at the RAD50 promoter and IFNγ promoter region were low but equivalent between control and MLL KD cells. These results indicate that the maintenance of histone modifications at the GATA3 locus and the Th2 cytokine gene loci is dependent upon the expression of MLL in the established Th2 cell lines.

The Binding of MLL to the GATA3 Gene Locus and the IL-4/IL-13 Gene Loci in Memory Th2 Cells

To search for target DNA regions where MLL protein is associated, we performed a ChIP-on-chip analysis in memory Th2 cells by means of a synthetic tiling microarray covering the GATA3 gene locus and the Th2 cytokine gene loci as described in the Experimental Procedures. The subtracted ratio values (MLL ChIP – control Ig ChIP) for each DNA spot (50 bp) around the GATA3 locus (top), the IL-4/IL-13 loci (middle), and IL-5 locus (bottom) are shown (Figure 6A). There were nine possible MLL binding regions around the GATA3 locus. These regions overlapped with the GATA3 promoter, exon2, intron2, intron3, and GATA3-CNS1 described in Figure 4. There were five possible binding regions around the IL-4/IL-13 loci and two in the IL-5 locus. These include the CGRE, CNS1, CNS2, and a ~2.5–3.0 Kb upstream region of IL-4 promoter. In order to examine the MLL binding more quantitatively, we performed a standard ChIP analysis with quantitative PCR and found that MLL binds to several sites in the GATA3 locus (promoter, exon2, and intron2) and to CGRE and CNS2 regions of the IL-4/IL-13 gene loci in memory Th2 cells (Figure 6B). No significant MLL accumulation was detected in either naive CD4 T cells or memory Th1 cells, suggesting that the binding for MLL is memory Th2 cell specific. Moreover, we compared the levels of MLL binding to the five selected regions indicated above between *MLL*$^{+/+}$ and *MLL*$^{+/-}$ memory Th2 cells, and as we expected, the levels were substantially reduced in *MLL*$^{+/-}$ memory Th2 cells (Figure 6C). These results indicate that MLL protein associates with some specific regions in the GATA3 locus and the IL-4/IL-13/IL-5 gene loci in memory Th2 cells.

The Expression of MLL Controls Memory Th2 Cell-Dependent Immune Responses and Inflammation In Vivo

The results thus far suggest that the expression levels of MLL control the ability to produce Th2 cytokines in

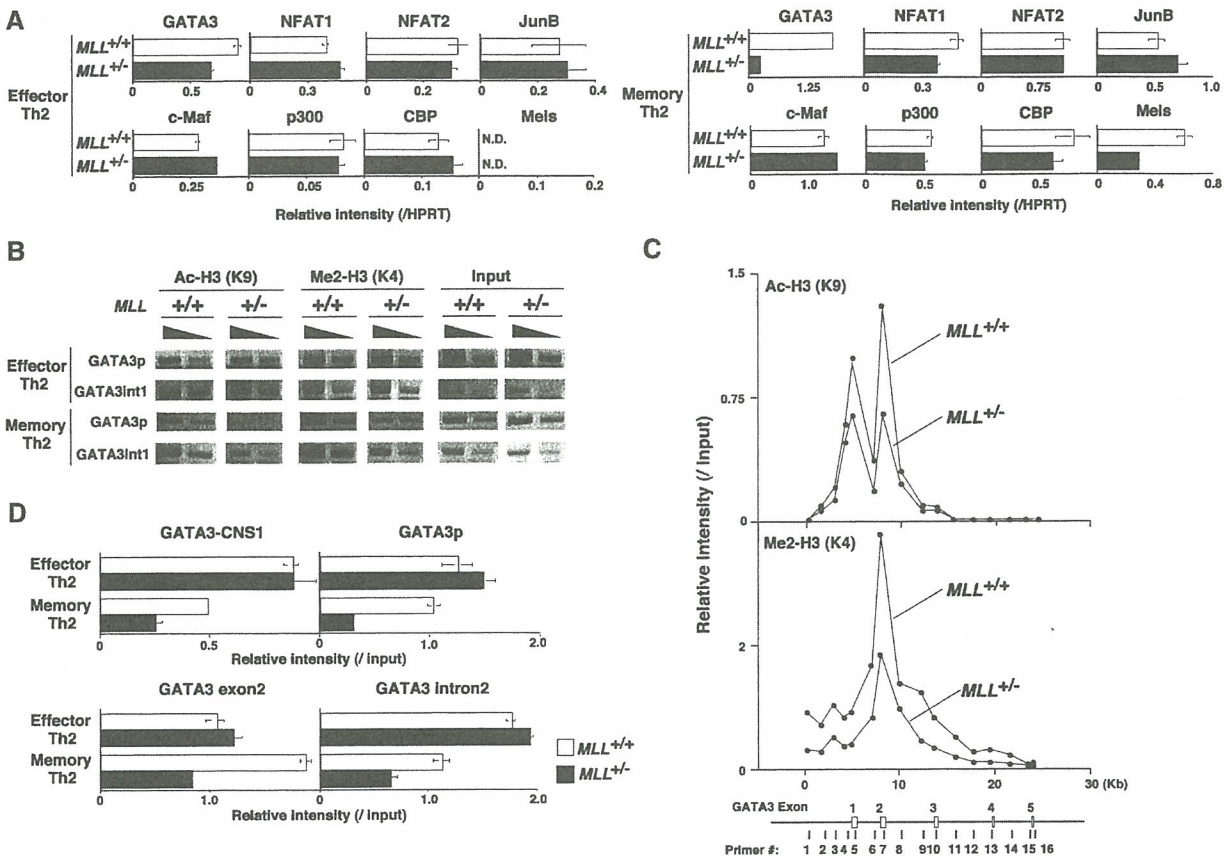

Figure 4. GATA3 Expression and Histone Modifications at the GATA3 Gene Locus in *MLL*$^{+/-}$ Memory Th2 Cells

(A) Decreased mRNA expression of GATA3 in *MLL*$^{+/-}$ memory Th2 cells. mRNA levels of GATA3, NFAT1, NFAT2, JunB, c-Maf, p300, CBP, Meis, and HPRT were determined by quantitative RT-PCR. The relative intensity (/HPRT) (mean of three samples) is shown with standard deviations. N.D., not detected.

(B) The acetylation of histone H3-K9 and methylation of histone H3-K4 at the GATA3 promoter and GATA3 intron1 region of the GATA3 gene locus in *MLL*$^{+/-}$ memory Th2 cells.

(C) A representative result of a ChIP analysis with a series of primer pairs covering the GATA3 locus. Shown is the relative intensity (/input) of each primer pair. The PCR product bands are shown in Figure S6. Three independent experiments were performed with similar results.

(D) The levels of methylation of histone H3-K4 at several regions around the GATA3 gene locus in *MLL*$^{+/-}$ memory Th2 cells was determined by a ChIP assay with a quantitative PCR analysis as described in Figure 2C. The regions examined are GATA3-CNS1 (location: approximately primer #2 site in [C]), GATA3 promoter (GATA3p, location: approximately primer #4 site in [C]), GATA3 exon2 (location: approximately primer #7 site in [C]), and GATA3 intron2 (location: approximately primer #8 site in [C]). The relative intensity (/input) (mean of three samples) is shown with standard deviations. Three independent experiments were performed with similar results.

memory Th2 cells. Therefore, we wished to examine the role for MLL in antigen-induced Th2-dependent inflammatory responses in vivo. The serum immunoglobulin concentrations (total and OVA-specific IgE, IgG1, IgG2a, and IgM) in memory Th2 mice after inhalation with OVA were measured. Substantial increases in the total and OVA-specific IgE and IgG1 (Th2-dependent isotypes) antibody production were observed after OVA inhalation in *MLL*$^{+/+}$ memory Th2 mice, but the level of increase significantly decreased in *MLL*$^{+/-}$ memory Th2 mice (Figure 7A). In contrast, the levels of Th1-dependent IgG2a were higher in the *MLL*$^{+/-}$ memory Th2 mice. The serum concentration of IgM was equivalent in both groups of mice.

Next, we looked at the levels of airway inflammation after OVA inhalation by examining infiltrating cells in harvested BAL fluid. The number of total infiltrating cells and the absolute numbers of eosinophils per mouse (Figure 7B, left) and the percentages of eosinophils (Figure 7B, right) decreased significantly in the *MLL*$^{+/-}$ memory Th2 mice. Representative staining profiles can be seen in Figure S7. In addition, the histological changes in the lungs of *MLL*$^{+/-}$ memory Th2 mice were evaluated by H&E staining (Figure 7C). The extent of inflammatory leukocyte infiltration in the peribronchiolar region was much less in the *MLL*$^{+/-}$ memory Th2 mice (Figure 7C). The infiltration of eosinophils in the lung as measured by Luna staining was, as expected, also significantly decreased in *MLL*$^{+/-}$ memory mice (data not shown). Mucus hyperproduction assessed by PAS staining was observed in wild-type memory Th2 mice, whereas the levels in *MLL*$^{+/-}$ memory Th2 mice dramatically decreased (Figure 7D). Taken together, these results indicate that the OVA-induced allergic eosinophilic inflammation was thus compromised in the *MLL*$^{+/-}$ memory Th2 mice. The methacholine-induced airway obstruction measured in a whole-body plethysmograph was significantly milder in the *MLL*$^{+/-}$ memory Th2 mice (data not shown).

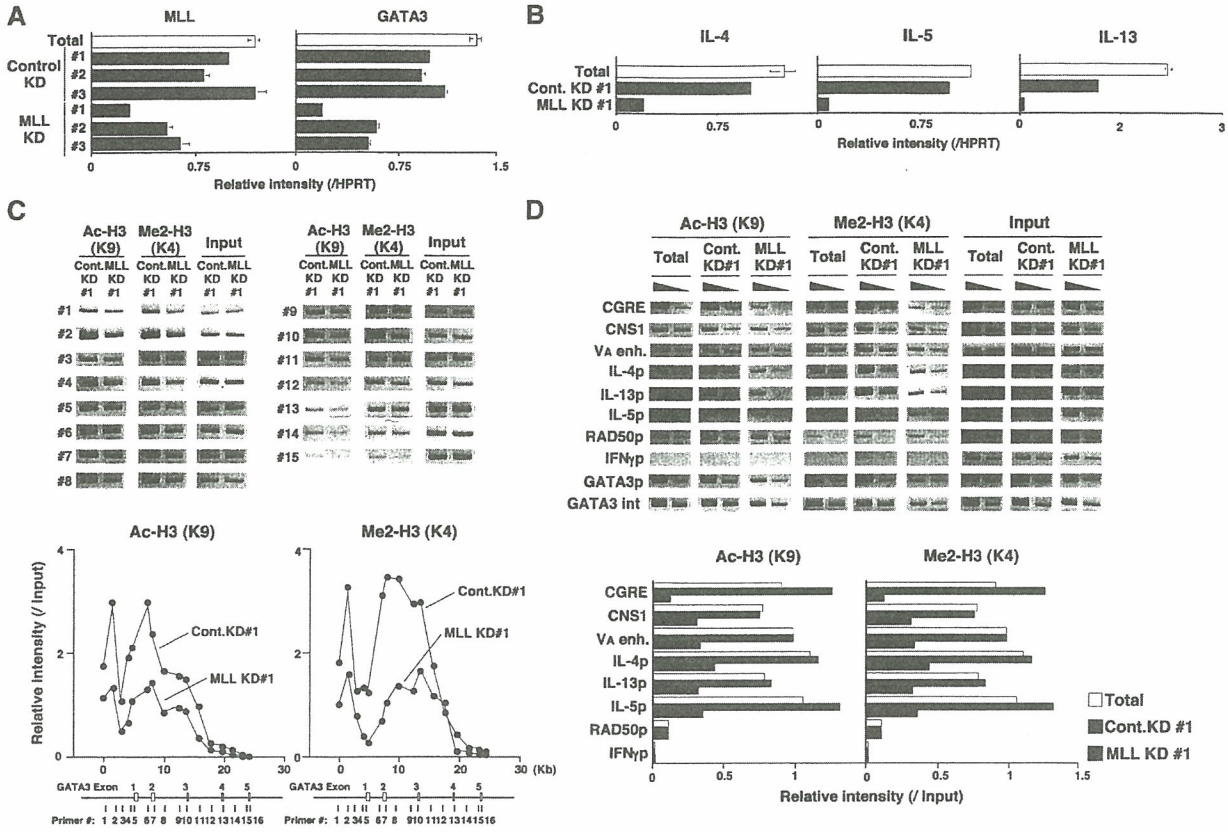

Figure 5. mRNA Expression and Histone Modification of the GATA3 Gene Locus and the Th2 Cytokine Gene Loci in *MLL*-Knockdown Th2 Cell Lines

(A) mRNA expression of MLL and GATA3 in *MLL*-knockdown (KD) Th2 cell lines (MLL KD #1, #2, and #3). mRNA levels of MLL, GATA3, and HPRT were determined by quantitative RT-PCR. The relative intensity (/HPRT) (mean of three samples) is shown with standard deviations. Total, D10G4.1 cells without selection.

(B) mRNA levels of IL-4, IL-5, IL-13, and HPRT in MLL KD #1 cells after PMA+Ionomycin stimulation (24 hr) were determined by quantitative RT-PCR. Relative intensity (/HPRT) (mean of three samples) is shown with standard deviations.

(C) Histone modifications within the GATA3 gene locus in MLL KD #1 cells. ChIP assay was performed with anti-acetylhistone H3-K9 and anti-dimethylhistone H3-K4 antibodies and the indicated specific primer pairs. Shown are the PCR product bands (top) and the relative intensity (/input) for each primer pair (bottom). Two independent experiments were performed with similar results.

(D) Histone modifications at the Th2 cytokine gene loci. PCR was performed with 3-fold serial dilution of template genomic DNA. Two independent experiments were performed with similar results.

Finally, we assessed the eosinophilic infiltration in $MLL^{+/+}$ and $MLL^{+/-}$ mice with DO11.10 Tg background. $MLL^{+/+}$ and $MLL^{+/-}$ mice were administered OVA twice intranasally on days 0 and 1, and 2 weeks later, mice were treated with inhaled OVA. As we expected, the level of eosinophilic infiltration was significantly milder in the $MLL^{+/-}$ mice (Figure 7E). These results indicate that the development of OVA-induced airway hyperresponsiveness was compromised in the $MLL^{+/-}$ mice.

Discussion

In this report, we demonstrate that MLL plays a crucial role in the regulation of the maintenance of Th2 identity in memory Th2 cells that was acquired during differentiation processes. MLL appears to regulate stable Th2 identity through the epigenetic control of the GATA3 locus and the Th2 cytokine gene loci in memory Th2 cells. The antigen-induced allergic airway inflammatory responses in vivo were compromised in $MLL^{+/-}$ memory Th2 mice, suggesting a physiological role for MLL in the regulation of allergic reactions.

Although the expression of GATA3 and the ability to produce Th2 cytokines are induced normally in $MLL^{+/-}$ effector Th2 cells, these Th2 features are not maintained properly in $MLL^{+/-}$ memory Th2 cells (Figure S4 and Figures 1B and 1C). Moreover, the hyperacetylation of histone H3-K9 and methylation of histone H3-K4 at the Th2 cytokine gene loci (Figure 2) and the GATA3 gene locus (Figures 4B–4D) that were normally induced in effector $MLL^{+/-}$ Th2 cells were not maintained properly in the memory Th2 cell stage. Furthermore, IL-4-producing $MLL^{+/-}$ effector Th2 cells failed to maintain the ability to produce Th2 cytokines and histone modifications under resting culture conditions in vitro (Figure 3). These findings are reminiscent of the notion that MLL protein is a functional homolog of *Drosophila melanogaster* trithorax, which is required for the maintenance but not for the initiation of *Hox* gene expression (Hanson et al., 1999; Yu et al., 1995, 1998). Such a cellular memory phenomenon is thought to be mediated through epigenetic mechanisms. MLL possesses an intrinsic histone methyl transferase (HMT) activity, which is mediated by the SET domain and specifically methylates histone H3-K4, an

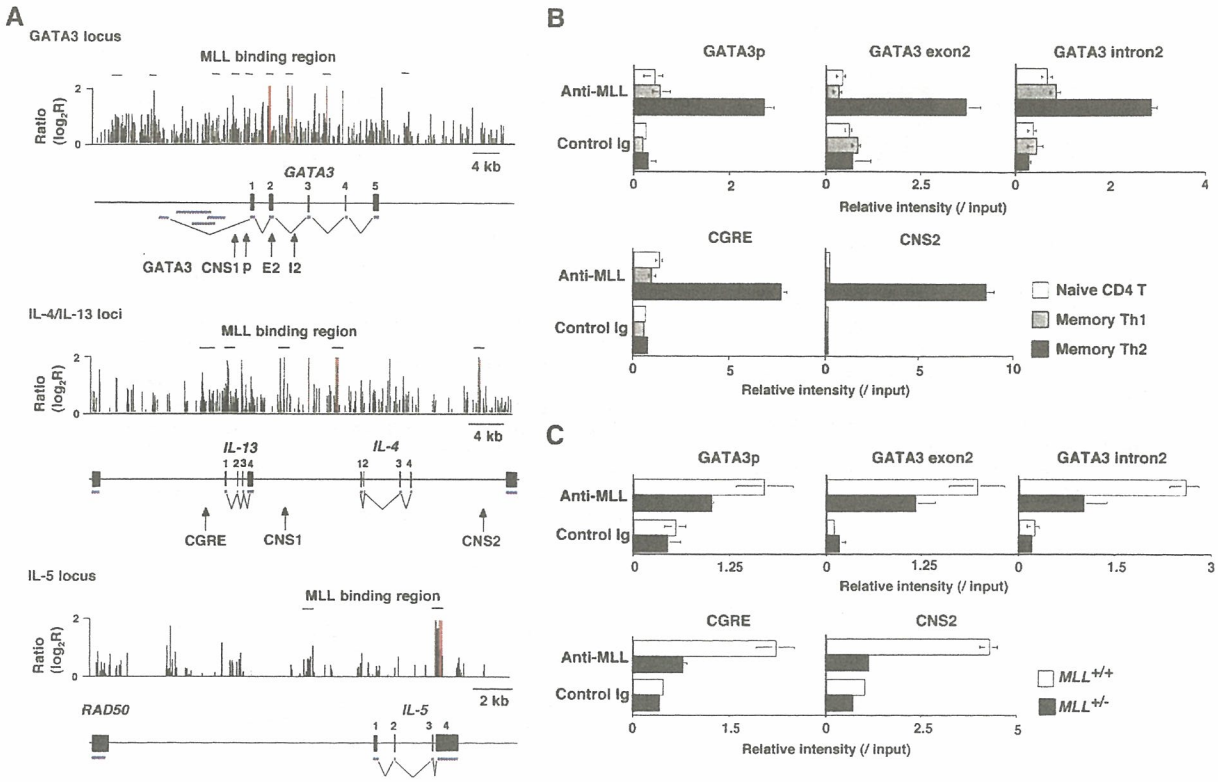

Figure 6. Binding of MLL Protein to Specific Regions around the GATA3 Gene Locus and the Th2 Cytokine Gene Loci

(A) A representative view of the results from MLL ChIP-on-chip analysis. The logarithmic ratio ($\log_2 R$) of hybridization intensities between MLL ChIP DNA and a control DNA was used. The subtracted ratio values (MLL ChIP – Control Ig ChIP) of each DNA spot (50 nucleotides) in the GATA3 locus (top), the IL-4/IL-13 loci (middle), and IL-5 locus (bottom) are shown. The red bars represent the values over 2. The horizontal bars represent possible MLL binding regions identified by a Signal Map Software. Reported transcripts (blue) are also shown.

(B) Standard ChIP assay with quantitative PCR for MLL. Naive CD4 T cells and memory Th1 and Th2 cells were used. The data for five selected regions (GATA3 promoter, GATA3 exon2, GATA3 intron2, CGRE, and CNS2) are shown. The relative intensity (/input) (mean of three samples) is shown with standard deviations.

(C) Decreased binding of MLL in *MLL*$^{+/-}$ memory Th2 cells. *MLL*$^{+/+}$ and *MLL*$^{+/-}$ memory Th2 cells were used. The relative intensity (/input) (mean of three samples) is shown with standard deviations.

epigenetic marker typically associated with transcriptionally active chromatin (Milne et al., 2002; Nakamura et al., 2002). In fact, we detected a notable decrease in the methylation of histone H3-K4 at the GATA3 gene locus and the Th2 cytokine gene loci in *MLL*$^{+/-}$ memory Th2 cells. Thus, it is likely that MLL regulates the maintenance of the Th2 phenotype in memory Th2 cells, in part through its HMT activity.

We and others previously reported that GATA3 expression is required for the production of Th2 cytokines in memory Th2 cells (Pai et al., 2004; Yamashita et al., 2004b; Zhu et al., 2004). The decreased expression of GATA3 mRNA (Figure 4A) and GATA3 protein (Figure S4) is observed in *MLL*$^{+/-}$ memory Th2 cells. The extent of histone modifications at the GATA3 locus was reduced in *MLL*$^{+/-}$ memory Th2 cells (Figures 4B–4D). Moreover, the introduction of exogenous GATA3 into *MLL*$^{+/-}$ memory Th2 cells partially restored the production of IL-4 (Figure S5). Thus, it is likely that the reduced capability to produce Th2 cytokines in *MLL*$^{+/-}$ memory Th2 cells is due at least in part to a decreased expression of GATA3 in *MLL*$^{+/-}$ memory Th2 cells.

A ChIP-on-chip analysis with anti-MLL antibody revealed nine possible MLL binding regions around the GATA3 locus (Figure 6A). These regions overlapped with the GATA3 promoter, exon2, intron2, intron3, and GATA3-CNS1 (an upstream conserved noncoding sequence; ~2.5–3.0 Kb upstream of the GATA3 exon1). There were five possible binding regions around the IL-4/IL-13 loci and two in the IL-5 locus. These included the CGRE, CNS1, CNS2, and a ~2.5–3.0 Kb upstream region of the IL-4 promoter. By using a standard ChIP analysis and quantitative PCR, we identified that MLL is associated with several GATA3 gene sites (promoter, exon2, and intron2), and the CGRE and CNS2 regions in the IL-4/IL-13 gene loci (Figure 6B). Interestingly, the MLL binding was highly specific for memory Th2 cells. Recently, the direct binding of MLL to nonmethylated CpG DNA sites has been reported (Ayton et al., 2004; Birke et al., 2002). The CXXC motif of MLL, which has homology with DNA binding sites of DNA methyl transferase 1 (DNMT1), is responsible for its binding to nonmethylated DNA (Ayton et al., 2004). The GATA3 exon2, CGRE, and CNS2 regions are highly G/C rich, and therefore a similar mechanism could be involved in the MLL binding to these regions in memory Th2 cells.

The second likely explanation for the reduction of Th2 cytokine production in *MLL*$^{+/-}$ memory Th2 cells is a defect in the direct epigenetic control of the Th2 cytokine gene locus by MLL. We identified at least two MLL

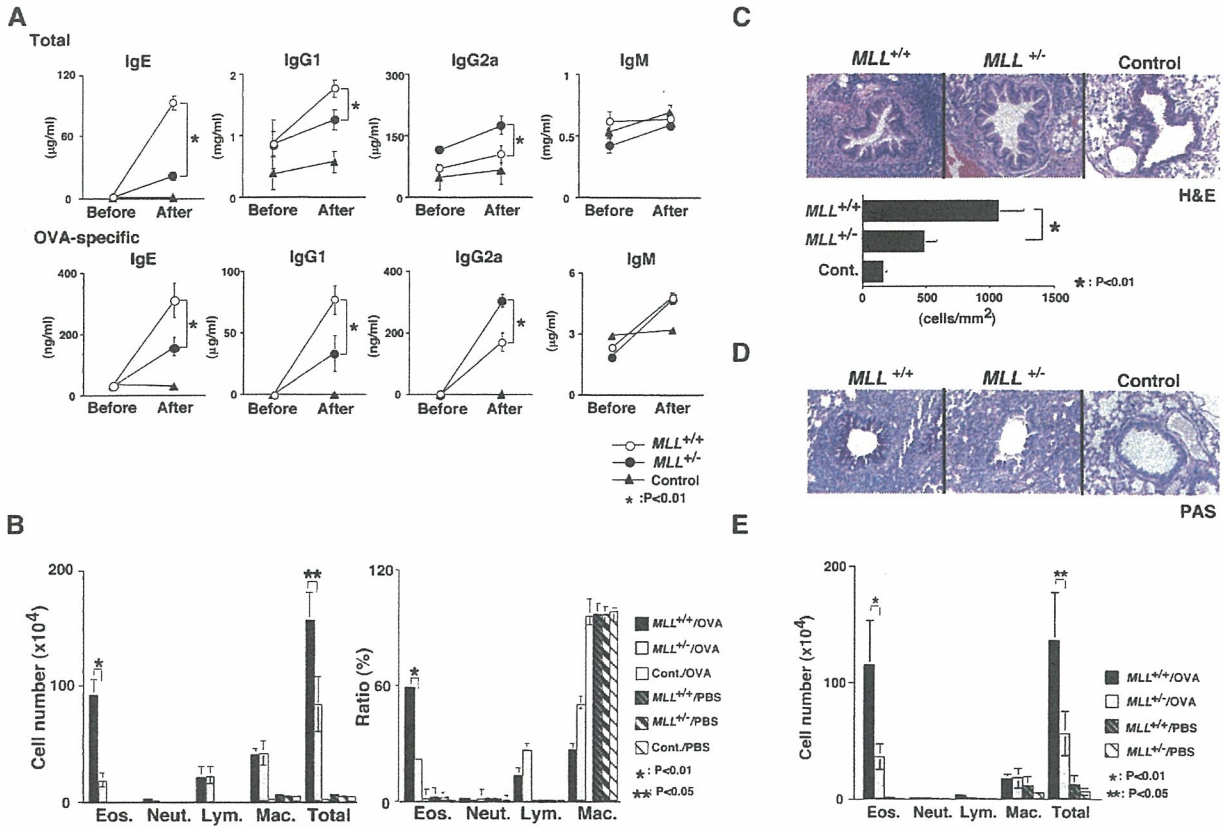

Figure 7. MLL Regulates the Memory Th2 Cell-Dependent Immune Responses and Inflammation In Vivo

OVA-specific wild-type ($MLL^{+/+}$) and $MLL^{+/-}$ effector Th2 cells with DO11.10 Tg background were intravenously transferred into BALB/c *nu/nu* mice. Five weeks after cell transfer, the mice were treated with inhaled OVA 4 times, on days 0, 2, 8, and 10.

(A) The serum concentrations of total (top) and OVA-specific (bottom) antibodies with the indicated isotype before (on day 0) and after (on day 11) OVA inhalation were determined by ELISA. The mean values with standard deviations (five animals per group) are shown. *$p < 0.01$ by Student's t test. The control represents BALB/c *nu/nu* mice without Th2 cell transfer.

(B) Reduced infiltration of eosinophils in bronchioalveolar lavage fluid (BAL) fluid. Memory Th2 mice were generated and inhaled with OVA as described above. BAL fluid was collected on day 12. The absolute cell number (left) and percentage (right) of eosinophils (Eos.), Neutrophils (Neut.), lymphocytes (Lym.), and macrophages (Mac.) in the BAL fluid are shown with standard deviations. Five mice per group were used. *$p < 0.01$; **$p < 0.05$ by Student's t test.

(C and D) On day 11, the lungs were fixed and stained with hematoxylin and eosin (H&E) (C) or with PAS (D). A representative staining pattern in each group is shown. Magnification, ×400. The number of infiltrated leukocytes in the peribronchiolar region (mean cell numbers/mm^2 with standard deviations) are also shown ([C], bottom). The control (Cont.) represents BALB/c *nu/nu* mice without Th2 cell transfer. *$p < 0.01$.

(E) Reduced infiltration of eosinophils in BAL fluid in $MLL^{+/-}$ mice. $MLL^{+/+}$ and $MLL^{+/-}$ mice with DO11.10 Tg background (five mice per group) were used. The results were obtained as described in [B]. *$p < 0.01$; **$p < 0.05$ by Student's t test.

binding sites within the IL-4/IL-13 gene loci in memory Th2 cells (CGRE and CNS2) (Figure 6). Since GATA3 is known to associate with these two regions in Th2 cells, MLL and GATA3 may colocalize and control the maintenance of histone modifications. In addition, we reported that RNA polymerase II (Pol II) complex was observed to accumulate selectively in the intergenic regions of the IL-13/IL-4 gene loci in memory Th2 cells (Yamashita et al., 2004a). Recently, the association of MLL with RNA polymerase II complex through the binding with Menin has been proposed (Milne et al., 2005; Yokoyama et al., 2004). Therefore, although more comprehensive biochemical studies are required, it is possible that MLL directly binds to the Th2 cytokine gene loci, thereby controlling the histone modifications and subsequent Th2 cytokine production in memory Th2 cells.

Allergic eosinophilic inflammation and airway hyperresponsiveness were compromised in $MLL^{+/-}$ memory Th2 mice (Figures 7A–7D). In this experimental asthma model, only the transferred effector Th2 cells have a defect in MLL expression and, therefore, any alteration observed would appear to be the consequence of defects in the transferred Th2 cells. It is thus likely that MLL controls asthmatic inflammation through the maintenance of the GATA3 expression and the production of Th2 cytokines in memory Th2 cells.

The Polycomb Group (PcG) family proteins antagonize the function of the Trithorax Group (trx-G) proteins by acting in a repressive manner on the target genes (Orlando et al., 1998). We previously reported that one of the PcG family protein, Mel-18, is involved in the induction of GATA3 expression and subsequent effector Th2 cell differentiation (Kimura et al., 2001). Although the precise molecular mechanisms underlying the Mel-18-mediated regulation of GATA3 expression have not yet been clarified, it is interesting to note that both groups of family proteins positively control the GATA3 expression at different stages in Th2 cells.

In summary, the results of this study indicate that MLL plays a crucial role in the control of the memory Th2 cell responses by maintaining the expression of GATA3 and the production of Th2 cytokines.

Experimental Procedures

Mice

Heterozygous MLL-deficient ($MLL^{+/-}$) mice were kindly provided by Dr. Toshihisa Komori (Nagasaki University, Japan) (Yagi et al., 1998). The animals used in this study were backcrossed to BALB/c 12 times. Anti-OVA-specific TCR-αβ (DO11.10) transgenic (Tg) mice were provided by Dr. D. Loh (Washington University School of Medicine, St. Louis, MO) (Murphy et al., 1990). $MLL^{+/-}$ × DO11.10 Tg mice were used at 6–8 weeks old. BALB/c and BALB/c *nu/nu* mice were purchased from Clea Inc., Tokyo, Japan. All mice used in this study were maintained under SPF conditions. Animal care was conducted in accordance with the guidelines of Chiba University.

Reagents

KJ-1-PE was prepared in our laboratory. For cytoplasmic staining, anti-IFNγ-FITC (XMG1.2) and anti-IL-4-PE (11B11) mAbs were used. Recombinant mouse IL-12 was purchased from BD-PharMingen and recombinant mouse IL-4 was from TOYOBO, Osaka, Japan. The OVA peptide (residues #323-339; ISQAVHAAHAEINEAGR) was synthesized by BEX Corporation, Tokyo, Japan.

The Generation of Effector and Memory Th1/Th2 Cells

Effector and memory Th1/Th2 cells were generated as previously described (Yamashita et al., 2004a). In brief, splenic CD4 T cells from DO11.10 OVA-specific TCR Tg mice were stimulated with an OVA peptide (Loh15, 1 μM) plus APC under the Th1- or Th2-culture conditions for 6 days in vitro. We used these cells as effector Th1 or Th2 cells, respectively. The effector Th1/Th2 cells (3×10^7) were transferred intravenously into BALB/c *nu/nu* recipient mice. In most of the experiments, 5 weeks after cell transfer, $KJ1^+$ cells in the spleen were purified by auto-MACS (Miltenyi Biotec) and then were used as memory Th1 and Th2 cells.

A Resting Culture System for Established Th2 Cells In Vitro

Naive CD4 T cells from $MLL^{+/-}$ × DO11.10 Tg mice were cultured under Th2 conditions for 6 days. The cultured cells were restimulated with anti-TCR mAb, and IL-4-producing cells (differentiated Th2 cells) in the culture were purified by the IL-4 secretion Assay kit (130-090-515, Militenyi Biotec) and flow cytometry sorting as described (Yamashita et al., 2004b). The purified IL-4-producing cells were further cultured in vitro for 7 days in the presence of IL-2 and anti-IL-4 mAb (11B.11), and then restimulated with OVA peptide and APC in the presence of anti-IL-4 mAb for additional 5 days. The second cycle of cultivation in the presence of anti-IL-4mAb allowed Th2 cells to rest more completely as evidenced by the phosphorylation levels of STAT6 (data not shown).

Quantitative RT-PCR

Quantitative RT-PCR was performed as described previously (Kimura et al., 2005). The primers for TaqMan probes for the detection of MLL (exon 11-12), GATA3, NFAT1, NFAT2, JunB, c-Maf, CBP, p300, Meis, IL-4, IL-5, IL-13, IFNγ, and HPRT were purchased from Applied Biosystems. The expression was normalized by the HPRT signal.

ELISA

Cytokine production and serum immunoglobulin concentrations were assessed by ELISA as described previously (Yamashita et al., 1999).

Immunoblotting

Immunoblotting was performed as described (Omori et al., 2003).

Chromatin Immunoprecipitation Assay

A ChIP assay was performed by ChIP assay kits (Upstate Biotechnology) as described (Yamashita et al., 2002). The specific primers and TaqMan probes used are described in the Supplemental Data. Anti-acetylhistone H3-K9 (ab4441) and anti-dimethylhistone H3-K4 (ab7766) antibodies were purchased from Abcam Co. (Cambridge, UK). Quantitative representations of the results are shown as relative band intensities measured by a densitometer.

ChIP-on-Chip Analysis

We first performed a standard ChIP on memory Th2 cells with anti-MLL antibody or normal rabbit IgG as a control. The generation of amplicons from the individual ChIP DNA sample was performed according to the manufactures' protocol (NimbleGen). In brief, sample DNA was blunted with T4 DNA polymerase (New England Biolabs) and ligated to the linker oligonucleotides (oligo-1: 5′-GCGGTG ACCCGGGAGATCTGAATTC-3′, oligo-2: 5′-GAATTCAGATC-3′) by means of T4 DNA ligase (New England Biolabs). Linker-ligated samples were amplified by PCR with oligo-1 probe as a primer, and PCR products were purified by Quiaquik PCR purification kit (QIAGEN). Oligonucleotide array analysis was performed by NimbleGen Systems as a part of a Chromatin Immunoprecipitation Array Service (NimbleGen). We used custom synthetic tiling microarrays containing the 2.5 Mb sequence around the Th2 cytokine gene loci and the 2.5 Mb sequence around the GATA3 gene locus. The probes (50 nucleotides, both the forward and reverse strands) designed to generate every 100 bases were printed at two random locations on the array. The logarithmic ratio ($\log_2 R$) of hybridization intensities between MLL ChIP DNA and a control DNA was calculated. The subtracted ratio values (MLL ChIP – Control Ig ChIP) of each DNA spot (50 nucleotides) were used. A possible binding region was identified by a Signal Map software.

Establishment of Stable MLL Knockdown Th2 Cell Lines

Stable MLL knockdown D10G4.1 cell lines were generated by pcPURmU6i cassette vector. In brief, stem loop type cDNA for MLL siRNA (sense: 5′-GTTTGCGTCAGGTTATAAAGCAAACGTGTG CTGTCCGTTTGCTTTGTAGCCTGATGCTTTTT-3′) was cloned into pcPURmU6i cassette vector, and the vector was transfected into D10G4.1 cells. Next the cells were cultured with Puromycin (4 μg/ml) for 4 weeks, and resistant cells were then picked up independently. The pcPURmU6i cassette vector containing GFP siRNA was used for the generation of stable control KD D10G4.1 cell lines.

Assessment of Memory Th2 Cell Functions In Vivo

OVA-specific wild-type and $MLL^{+/-}$ effector Th2 cells were intravenously transferred into BALB/c *nu/nu* mice. Five weeks after transfer, the mice were treated with inhaled 1% of OVA 4 times, on days 0, 2, 8, and 10. The serum immunoglobulin levels and lung histology were then assessed on day 11 as described previously (Kamata et al., 2003). BAL fluid was collected on day 12. In some experiments, $MLL^{+/-}$ mice with a DO11.10 Tg background were administered OVA (100 μg/35 μl) twice intranasally, on days 0 and 1. On day 14, the mice were treated with inhaled 1% of OVA, and BAL fluid was collected on day 16.

Supplemental Data

Supplemental Data include seven figures and Supplemental Experimental Procedures and can be found with this article online at http://www.immunity.com/cgi/content/full/24/5/611/DC1/.

Acknowledgments

The authors are grateful to Drs. Ralph T. Kubo, Atsushi Iwama, Kenzo Hiroshima, and Erwin Gelfand for helpful comments and constructive criticisms in the preparation of the manuscript. We thank Drs. Toshihisa Komori and Haruhiko Koseki for mll-deficient mice. We thank Ms. Hikari Asou and Kaoru Sugaya for their excellent technical assistance. This work was supported by grants from the Ministry of Education, Culture, Sports, Science, and Technology (Japan) (Grants-in-Aid for: Scientific Research in Priority Areas #17016010 and #17047007; Scientific Research B #17390139, Scientific Research C #18590466; Grant-in-Aid for Young Scientists #17790318, and Special Coordination Funds for Promoting Science and Technology), the Ministry of Health, Labor, and Welfare (Japan), the Program for Promotion of Fundamental Studies in Health Sciences of the National Institute of Biomedical Immovation (Japan), The Japan

Health Science Foundation, Kanae Foundation, Uehara Memorial Foundation, and Mochida Foundation.

Received: September 13, 2005
Revised: February 28, 2006
Accepted: March 3, 2006
Published: May 23, 2006

References

Agarwal, S., Avni, O., and Rao, A. (2000). Cell-type-restricted binding of the transcription factor NFAT to a distal IL-4 enhancer in vivo. Immunity *12*, 643–652.

Ansel, K.M., Lee, D.U., and Rao, A. (2003). An epigenetic view of helper T cell differentiation. Nat. Immunol. *4*, 616–623.

Avni, O., Lee, D., Macian, F., Szabo, S.J., Glimcher, L.H., and Rao, A. (2002). T_H cell differentiation is accompanied by dynamic changes in histone acetylation of cytokine genes. Nat. Immunol. *3*, 643–651.

Ayton, P.M., Chen, E.H., and Cleary, M.L. (2004). Binding to nonmethylated CpG DNA is essential for target recognition, transactivation, and myeloid transformation by an MLL oncoprotein. Mol. Cell. Biol. *24*, 10470–10478.

Birke, M., Schreiner, S., Garcia-Cuellar, M.P., Mahr, K., Titgemeyer, F., and Slany, R.K. (2002). The MT domain of the proto-oncoprotein MLL binds to CpG-containing DNA and discriminates against methylation. Nucleic Acids Res. *30*, 958–965.

Constant, S.L., and Bottomly, K. (1997). Induction of Th1 and Th2 $CD4^+$ T cell responses: the alternative approaches. Annu. Rev. Immunol. *15*, 297–322.

Dutton, R.W., Bradley, L.M., and Swain, S.L. (1998). T cell memory. Annu. Rev. Immunol. *16*, 201–223.

Ernst, P., Fisher, J.K., Avery, W., Wade, S., Foy, D., and Korsmeyer, S.J. (2004). Definitive hematopoiesis requires the *mixed-lineage leukemia* gene. Dev. Cell *6*, 437–443.

Fields, P.E., Kim, S.T., and Flavell, R.A. (2002). Cutting edge: changes in histone acetylation at the *IL-4* and *IFN-γ* loci accompany Th1/Th2 differentiation. J. Immunol. *169*, 647–650.

Francis, N.J., and Kingston, R.E. (2001). Mechanisms of transcriptional memory. Nat. Rev. Mol. Cell Biol. *2*, 409–421.

Gu, Y., Nakamura, T., Alder, H., Prasad, R., Canaani, O., Cimino, G., Croce, C.M., and Canaani, E. (1992). The t(4;11) chromosome translocation of human acute leukemias fuses the ALL-1 gene, related to *Drosophila* trithorax, to the AF-4 gene. Cell *71*, 701–708.

Hanson, R.D., Hess, J.L., Yu, B.D., Ernst, P., van Lohuizen, M., Berns, A., van der Lugt, N.M., Shashikant, C.S., Ruddle, F.H., Seto, M., and Korsmeyer, S.J. (1999). Mammalian *Trithorax* and *polycomb*-group homologues are antagonistic regulators of homeotic development. Proc. Natl. Acad. Sci. USA *96*, 14372–14377.

Hess, J.L., Yu, B.D., Li, B., Hanson, R., and Korsmeyer, S.J. (1997). Defects in yolk sac hematopoiesis in *Mll*-null embryos. Blood *90*, 1799–1806.

Jameson, S.C. (2002). Maintaining the norm: T-cell homeostasis. Nat. Rev. Immunol. *2*, 547–556.

Kamata, T., Yamashita, M., Kimura, M., Murata, K., Inami, M., Shimizu, C., Sugaya, K., Wang, C.R., Taniguchi, M., and Nakayama, T. (2003). *src* homology 2 domain-containing tyrosine phosphatase SHP-1 controls the development of allergic airway inflammation. J. Clin. Invest. *111*, 109–119.

Kimura, M., Koseki, Y., Yamashita, M., Watanabe, N., Shimizu, C., Katsumoto, T., Kitamura, T., Taniguchi, M., Koseki, H., and Nakayama, T. (2001). Regulation of Th2 cell differentiation by *mel-18*, a mammalian *polycomb* group gene. Immunity *15*, 275–287.

Kimura, M.Y., Hosokawa, H., Yamashita, M., Hasegawa, A., Iwamura, C., Watarai, H., Taniguchi, M., Takagi, T., Ishii, S., and Nakayama, T. (2005). Regulation of T helper type 2 cell differentiation by murine Schnurri-2. J. Exp. Med. *201*, 397–408.

Kondrack, R.M., Harbertson, J., Tan, J.T., McBreen, M.E., Surh, C.D., and Bradley, L.M. (2003). Interleukin 7 regulates the survival and generation of memory CD4 cells. J. Exp. Med. *198*, 1797–1806.

Krumlauf, R. (1994). Hox genes in vertebrate development. Cell *78*, 191–201.

Lee, H.J., Takemoto, N., Kurata, H., Kamogawa, Y., Miyatake, S., O'Garra, A., and Arai, N. (2000). GATA-3 induces T helper cell type 2 (Th2) cytokine expression and chromatin remodeling in committed Th1 cells. J. Exp. Med. *192*, 105–115.

Li, J., Huston, G., and Swain, S.L. (2003). IL-7 promotes the transition of CD4 effectors to persistent memory cells. J. Exp. Med. *198*, 1807–1815.

Lohning, M., Richter, A., and Radbruch, A. (2002). Cytokine memory of T helper lymphocytes. Adv. Immunol. *80*, 115–181.

Loots, G.G., Locksley, R.M., Blankespoor, C.M., Wang, Z.E., Miller, W., Rubin, E.M., and Frazer, K.A. (2000). Identification of a coordinate regulator of interleukins *4*, 13, and 5 by cross-species sequence comparisons. Science *288*, 136–140.

Milne, T.A., Briggs, S.D., Brock, H.W., Martin, M.E., Gibbs, D., Allis, C.D., and Hess, J.L. (2002). MLL targets SET domain methyltransferase activity to *Hox* gene promoters. Mol. Cell *10*, 1107–1117.

Milne, T.A., Hughes, C.M., Lloyd, R., Yang, Z., Rozenblatt-Rosen, O., Dou, Y., Schnepp, R.W., Krankel, C., Livolsi, V.A., Gibbs, D., et al. (2005). Menin and MLL cooperatively regulate expression of cyclin-dependent kinase inhibitors. Proc. Natl. Acad. Sci. USA *102*, 749–754.

Mosmann, T.R., Cherwinski, H., Bond, M.W., Giedlin, M.A., and Coffman, R.L. (1986). Two types of murine helper T cell clone. I. Definition according to profiles of lymphokine activities and secreted proteins. J. Immunol. *136*, 2348–2357.

Murphy, K.M., Heimberger, A.B., and Loh, D.Y. (1990). Induction by antigen of intrathymic apoptosis of $CD4^+CD8^+TCR^{lo}$ thymocytes in vivo. Science *250*, 1720–1723.

Murphy, K.M., Ouyang, W., Farrar, J.D., Yang, J., Ranganath, S., Asnagli, H., Afkarian, M., and Murphy, T.L. (2000). Signaling and transcription in T helper development. Annu. Rev. Immunol. *18*, 451–494.

Nakamura, T., Mori, T., Tada, S., Krajewski, W., Rozovskaia, T., Wassell, R., Dubois, G., Mazo, A., Croce, C.M., and Canaani, E. (2002). ALL-1 is a histone methyltransferase that assembles a supercomplex of proteins involved in transcriptional regulation. Mol. Cell *10*, 1119–1128.

Nelms, K., Keegan, A.D., Zamorano, J., Ryan, J.J., and Paul, W.E. (1999). The IL-4 receptor: signaling mechanisms and biologic functions. Annu. Rev. Immunol. *17*, 701–738.

O'Garra, A. (1998). Cytokines induce the development of functionally heterogeneous T helper cell subsets. Immunity *8*, 275–283.

Omori, M., Yamashita, M., Inami, M., Ukai-Tadenuma, M., Kimura, M., Nigo, Y., Hosokawa, H., Hasegawa, A., Taniguchi, M., and Nakayama, T. (2003). CD8 T cell-specific downregulation of histone hyperacetylation and gene activation of the IL-4 gene locus by ROG, repressor of GATA. Immunity *19*, 281–294.

Orlando, V., Jane, E.P., Chinwalla, V., Harte, P.J., and Paro, R. (1998). Binding of trithorax and Polycomb proteins to the bithorax complex: dynamic changes during early *Drosophila* embryogenesis. EMBO J. *17*, 5141–5150.

Pai, S.Y., Truitt, M.L., and Ho, I.C. (2004). GATA-3 deficiency abrogates the development and maintenance of T helper type 2 cells. Proc. Natl. Acad. Sci. USA *101*, 1993–1998.

Popovic, R., and Zeleznik-Le, N.J. (2005). MLL: how complex does it get? J. Cell. Biochem. *95*, 234–242.

Reiner, S.L., and Locksley, R.M. (1995). The regulation of immunity to *Leishmania major*. Annu. Rev. Immunol. *13*, 151–177.

Schluns, K.S., and Lefrancois, L. (2003). Cytokine control of memory T-cell development and survival. Nat. Rev. Immunol. *3*, 269–279.

Seddon, B., Tomlinson, P., and Zamoyska, R. (2003). Interleukin 7 and T cell receptor signals regulate homeostasis of CD4 memory cells. Nat. Immunol. *4*, 680–686.

Seder, R.A., and Paul, W.E. (1994). Acquisition of lymphokine-producing phenotype by $CD4^+$ T cells. Annu. Rev. Immunol. *12*, 635–673.

Sprent, J., and Surh, C.D. (2002). T cell memory. Annu. Rev. Immunol. *20*, 551–579.

Szabo, S.J., Kim, S.T., Costa, G.L., Zhang, X., Fathman, C.G., and Glimcher, L.H. (2000). A novel transcription factor, T-bet, directs Th1 lineage commitment. Cell *100*, 655–669.

Thirman, M.J., Gill, H.J., Burnett, R.C., Mbangkollo, D., McCabe, N.R., Kobayashi, H., Ziemin-van der Poel, S., Kaneko, Y., Morgan, R., Sandberg, A.A., et al. (1993). Rearrangement of the MLL gene in acute lymphoblastic and acute myeloid leukemias with 11q23 chromosomal translocations. N. Engl. J. Med. *329*, 909–914.

Tkachuk, D.C., Kohler, S., and Cleary, M.L. (1992). Involvement of a homolog of *Drosophila* trithorax by 11q23 chromosomal translocations in acute leukemias. Cell *71*, 691–700.

Yagi, H., Deguchi, K., Aono, A., Tani, Y., Kishimoto, T., and Komori, T. (1998). Growth disturbance in fetal liver hematopoiesis of Mll-mutant mice. Blood *92*, 108–117.

Yamashita, M., Hashimoto, K., Kimura, M., Kubo, M., Tada, T., and Nakayama, T. (1998). Requirement for $p56^{lck}$ tyrosine kinase activation in T_h subset differentiation. Int. Immunol. *10*, 577–591.

Yamashita, M., Kimura, M., Kubo, M., Shimizu, C., Tada, T., Perlmutter, R.M., and Nakayama, T. (1999). T cell antigen receptor-mediated activation of the Ras/mitogen-activated protein kinase pathway controls interleukin 4 receptor function and type-2 helper T cell differentiation. Proc. Natl. Acad. Sci. USA *96*, 1024–1029.

Yamashita, M., Katsumata, M., Iwashima, M., Kimura, M., Shimizu, C., Kamata, T., Shin, T., Seki, N., Suzuki, S., Taniguchi, M., and Nakayama, T. (2000). T cell receptor-induced calcineurin activation regulates T helper type 2 cell development by modifying the interleukin 4 receptor signaling complex. J. Exp. Med. *191*, 1869–1879.

Yamashita, M., Ukai-Tadenuma, M., Kimura, M., Omori, M., Inami, M., Taniguchi, M., and Nakayama, T. (2002). Identification of a conserved GATA3 response element upstream proximal from the interleukin-13 gene locus. J. Biol. Chem. *277*, 42399–42408.

Yamashita, M., Shinnakasu, R., Nigo, Y., Kimura, M., Hasegawa, A., Taniguchi, M., and Nakayama, T. (2004a). Interleukin (IL)-4-independent maintenance of histone modification of the IL-4 gene loci in memory Th2 cells. J. Biol. Chem. *279*, 39454–39464.

Yamashita, M., Ukai-Tadenuma, M., Miyamoto, T., Sugaya, K., Hosokawa, H., Hasegawa, A., Kimura, M., Taniguchi, M., DeGregori, J., and Nakayama, T. (2004b). Essential role of GATA3 for the maintenance of type 2 helper T (Th2) cytokine production and chromatin remodeling at the Th2 cytokine gene loci. J. Biol. Chem. *279*, 26983–26990.

Yamashita, M., Shinnakasu, R., Asou, H., Kimura, M., Hasegawa, A., Hashimoto, K., Hatano, N., Ogata, M., and Nakayama, T. (2005). Ras-ERK MAPK cascade regulates GATA3 stability and Th2 differentiation through ubiquitin-proteasome pathway. J. Biol. Chem. *280*, 29409–29419.

Yokoyama, A., Wang, Z., Wysocka, J., Sanyal, M., Aufiero, D.J., Kitabayashi, I., Herr, W., and Cleary, M.L. (2004). Leukemia proto-oncoprotein MLL forms a SET1-like histone methyltransferase complex with menin to regulate *Hox* gene expression. Mol. Cell. Biol. *24*, 5639–5649.

Yu, B.D., Hess, J.L., Horning, S.E., Brown, G.A., and Korsmeyer, S.J. (1995). Altered Hox expression and segmental identity in *Mll*-mutant mice. Nature *378*, 505–508.

Yu, B.D., Hanson, R.D., Hess, J.L., Horning, S.E., and Korsmeyer, S.J. (1998). MLL, a mammalian *trithorax*-group gene, functions as a transcriptional maintenance factor in morphogenesis. Proc. Natl. Acad. Sci. USA *95*, 10632–10636.

Zhang, D.H., Cohn, L., Ray, P., Bottomly, K., and Ray, A. (1997). Transcription factor GATA-3 is differentially expressed in murine Th1 and Th2 cells and controls Th2-specific expression of the interleukin-5 gene. J. Biol. Chem. *272*, 21597–21603.

Zheng, W., and Flavell, R.A. (1997). The transcription factor GATA-3 is necessary and sufficient for Th2 cytokine gene expression in CD4 T cells. Cell *89*, 587–596.

Zhu, J., Min, B., Hu-Li, J., Watson, C.J., Grinberg, A., Wang, Q., Killeen, N., Urban, J.F., Jr., Guo, L., and Paul, W.E. (2004). Conditional deletion of *Gata3* shows its essential function in T_H1-T_H2 responses. Nat. Immunol. *5*, 1157–1165.

Ziemin-van der Poel, S., McCabe, N.R., Gill, H.J., Espinosa, R., III, Patel, Y., Harden, A., Rubinelli, P., Smith, S.D., LeBeau, M.M., Rowley, J.D., et al. (1991). Identification of a gene, *MLL*, that spans the breakpoint in 11q23 translocations associated with human leukemias. Proc. Natl. Acad. Sci. USA *88*, 10735–10739.

Regulation of allergic airway inflammation through Toll-like receptor 4-mediated modification of mast cell function

Yukiko I. Nigo*†, Masakatsu Yamashita*†, Kiyoshi Hirahara*, Ryo Shinnakasu*, Masamichi Inami*, Motoko Kimura*, Akihiro Hasegawa*, Yoichi Kohno‡, and Toshinori Nakayama*§

Departments of *Immunology and ‡Pediatrics, Graduate School of Medicine, Chiba University, 1-8-1 Inohana Chuo-ku, Chiba 260-8670, Japan

Communicated by K. Frank Austen, Harvard Medical School, Boston, MA, December 19, 2005 (received for review April 19, 2005)

In a mouse experimental asthma model, the administration of bacterial lipopolysaccharide (LPS), particularly at low doses, enhances the levels of ovalbumin (OVA)-induced eosinophilic airway inflammation. In an effort to clarify the cellular and molecular basis for the LPS effect, we demonstrate that the OVA-induced eosinophilic inflammation in the lung is dramatically increased by the administration of LPS in wild-type mice, whereas such increase was not observed in mast-cell-deficient mice or Toll-like receptor (TLR)4-deficient mice. Adoptive transfer of bone-marrow-derived mast cells (BMMCs) from wild-type, but not from TLR4-deficient, mice restored the increased eosinophilic inflammation in mast-cell-deficient mice. Wild-type BMMCs pretreated with LPS *in vitro* also reconstituted the eosinophilic inflammation. Moreover, *in vitro* analysis revealed that the treatment of BMMCs with LPS resulted in NF-κB activation, sustained up-regulation of GATA1 and -2 expression, and increased the capability to produce IL-5 and -13. Dramatic increases in the expression of IL-5 and -13 and Eotaxin 2 were detected in LPS-treated BMMCs after costimulation with LPS and IgE/Ag. Overexpression of GATA1, but not GATA2, in MC9 mast cells resulted in increased transcriptional activity of IL-4, -5, and -13. Furthermore, the levels of transcription of Th2 cytokines in BMMCs were decreased by the introduction of small interfering RNA for GATA1. Thus, mast cells appear to control allergic airway inflammation after their activation and modulation through TLR4-mediated induction of GATA1 and subsequent increase in Th2 cytokine production.

cytokine | GATA1 | mast cell | lipopolysaccharide | bone-marrow-derived mast cells

It is well established that mast cells play a central role in anaphylactic reactions. Mast cells are activated by multivalent binding of antigens to receptor-bound IgE and release inflammatory mediators, such as histamine, prostaglandins, and leukotrienes (1–5). It is also known that mast cells regulate the levels of allergic inflammatory responses in the airways by producing cytokines, such as IL-4, -5, -6, -10, and -13 and TNF-α, which are important in the pathogenesis of various allergic reactions (6, 7). In particular, IL-5 production is reported to be critical for the pathogenesis of eosinophilic infiltration in the lung (8, 9).

It is well recognized that respiratory infection modulates allergic airway inflammation (10). However, as for the role for exposure of bacterial components such as lipopolysaccharide (LPS) in allergic inflammation, there is apparent controversy, as evidenced by studies suggesting protective roles for LPS through Th1 cell induction and studies showing the exacerbating effects of LPS on asthma (11–13). LPS, a major component of the outer membrane of Gram-negative bacteria, is ubiquitously distributed in the environment, including household dusts. Recently, Th1/Th2 inflammatory responses were reported to be influenced by the levels of LPS exposure (14). The exposure to high-level LPS with antigens resulted in increased antigen-specific Th1 responses, whereas a low dose of LPS resulted in Th2 sensitization. Collectively, these results suggest a unique biphasic effect for LPS in allergic inflammatory responses.

Recent progress has revealed that innate immune responses are initiated by various pattern-recognition receptors, Toll-like receptors (TLRs) (15). TLRs comprise a family of proteins that enhance certain cytokine gene transcription in response to various pathogenic ligands and control acquired immune responses such as Th1 responses (16, 17). TLR4 was shown to be a receptor for LPS (18, 19). Recent studies on mouse (20–22) and human (23) mast cells suggested that LPS-induced activation was mediated through TLR4 expressed on mast cells. A protective role for mast cells in bacterial infection was first addressed in a bacterial peritonitis animal model, and the infection was suggested to be mediated by the production of TNFα as a consequence of TLR4 activation (21, 24, 25). More recently, LPS-induced production of inflammatory cytokines (IL-1β, TNF-α, IL-6, and IL-13) from mast cells in the peritoneal cavity and the resulting neutrophil recruitment were suggested to be important for protection in septic peritonitis (26). In addition, TNFα produced by mast cells was reported to be involved in hypertrophy of draining lymph nodes during intradermal bacterial infection (27). However, the consequences of LPS-induced mast-cell activation in allergic airway inflammation have not been well elucidated.

In this study, we investigated the role of TLR4 on mast cells in allergic airway inflammation using mast-cell-deficient W/W^v mice and TLR4-deficient [knockout (KO)] mice. The dramatic enhancement of eosinophilic airway inflammation induced by coadministration of a low-dose LPS and ovalbumin (OVA) at the priming phase in wild-type mice was not observed in W/W^v mice. Cell-transfer experiments using TLR4 KO mast cells indicated that the effect of LPS is mediated through TLR4 on mast cells. Furthermore, we demonstrate that bone-marrow-derived mast cells (BMMCs) cultured with LPS for 1 week show an augmented ability to produce Th2 cytokines, which may help explain the enhancement of allergic eosinophilic airway inflammation.

Results

LPS-Mediated Enhancement of Eosinophilic Inflammation Is Not Observed in W/W^v Mice. The goal of this study was to clarify molecular targets for LPS in mast-cell activation and allergic eosinophilic airway inflammation. First, we examined the effect of LPS on

---

Conflict of interest statement: No conflicts declared.

Freely available online through the PNAS open access option.

Abbreviations: BAL, bronchoalveolar lavage; BMMC, bone-marrow-derived mast cell; DC, dendritic cell; H.E., hematoxylin and eosin; KO, knockout; LPS, lipopolysaccharide; OVA, ovalbumin; PMA, phorbol 12-myristate 13-acetate; siRNA, small interfering RNA; TLR, Toll-like receptor.

†Y.I.N. and M.Y. contributed equally to this work.

§To whom correspondence should be addressed at: Department of Immunology (H3), Graduate School of Medicine, Chiba University, 1-8-1 Inohana, Chuo-ku, Chiba 260-8670, Japan. E-mail: tnakayama@faculty.chiba-u.jp.

www.pnas.org/cgi/doi/10.1073/pnas.0510685103

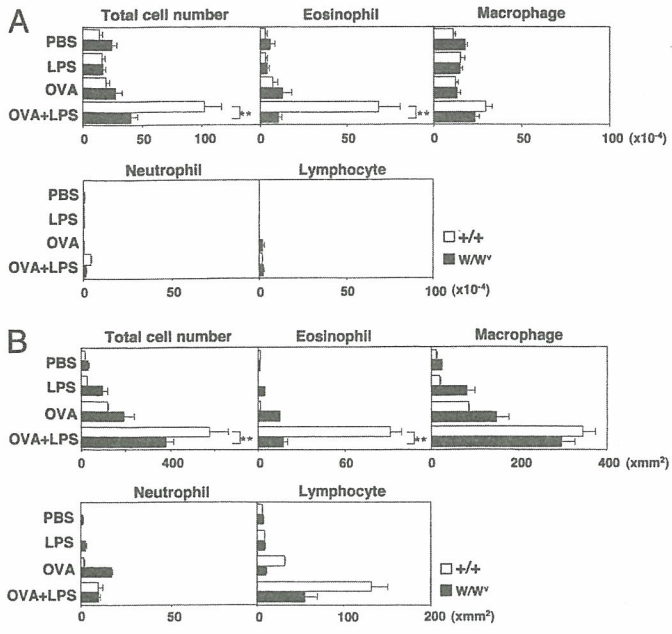

Fig. 1. LPS-mediated enhancement of eosinophilic inflammation was not observed in W/W^v mice. Wild-type (+/+) and mast-cell-deficient (W/W^v) mice were immunized with OVA (10 μg) in conjunction with 1 μg of LPS intranasally, and, 2 weeks later, OVA (25 μg) was again administrated intranasally. (*A*) One day after the final OVA administration, BAL fluid was harvested and examined for infiltrating cells. Mean values, with standard deviation, of the numbers of total cells and each cell type are shown. Ten mice were used in each group. **, <0.01 (Dunnett multiple comparisons test). (*B*) Histological examination was done 2 days after the final OVA administration. Mean values, with standard deviation, of the numbers of infiltrated leukocytes in 1 mm^2 are shown. Ten lung sections per mouse from three mice in each group were examined. **, <0.01 (Dunnett multiple comparisons test).

OVA-induced allergic airway inflammation. Wild-type (+/+) and mast-cell-deficient W/W^v mice were treated intranasally with soluble OVA (10 μg) in conjunction with low-dose LPS (1 μg), and, 2 weeks later, the mice were challenged intranasally with OVA (25 μg). Under these conditions, Th2-skewed eosinophilic inflammation was reproducibly induced in the lung (14). Two days after the final OVA challenge, bronchoalveolar lavage (BAL) fluid was harvested and examined for infiltrating leukocytes. A summary of the types of infiltrating cells is shown in Fig. 1*A*, and a representative photographic view of May–Giemsa staining in each group can be seen in Fig. 5, which is published as supporting information on the PNAS web site. A modest (≈2-fold) but reproducible increase in the number of eosinophils was detected in mice treated with OVA alone as compared with those in PBS- or LPS-treated mice. The extent of eosinophilic infiltration induced in this protocol was significantly lower than that induced by intraperitoneal immunization of OVA with alum (data not shown) (28, 29). However, the numbers of total cells and eosinophils were significantly increased when wild-type +/+ mice were treated with both OVA and LPS. Intriguingly, when W/W^v mice were treated with OVA plus LPS, the numbers of total infiltrating cells and eosinophils did not increase significantly, as compared with those in +/+ mice. These results point to an important role for mast cells in LPS-mediated enhancement of eosinophilic infiltration in BAL fluid. Furthermore, the expression of Th2 cytokines (IL-4, -5, and -13) and Eotaxin-2 in the BAL fluid of wild-type +/+ and W/W^v mice was examined, and significantly decreased expression was detected in the case of W/W^v mice (see Fig. 6, which is published as supporting information on the PNAS web site).

Concurrently, changes in lung histology were examined. A summary of the numbers of infiltrating leukocytes calculated by using hematoxylin and eosin (H.E.) staining and Luna staining for eosinophils is shown in Fig. 1*B*. Among the leukocytes infiltrating, the number of eosinophils was increased dramatically when LPS was coadministered to wild-type mice, and the LPS effect was not observed in W/W^v mice. Sections with H.E. staining can be seen in Fig. 7, which is published as supporting information on the PNAS web site, and Luna staining in Fig. 8, which is published as supporting information on the PNAS web site. Moreover, Masson–trichrome staining revealed substantial levels of subepithelial fibrosis (stained by blue dye) in +/+ mice immunized with OVA plus LPS (see Fig. 9*d*, which is published as supporting information on the PNAS web site). In W/W^v mice, however, basically no significant fibrosis was detected. Thus, mast cells play a crucial role in low-dose LPS-mediated enhancement of eosinophilic airway inflammation induced by OVA.

Adoptive Transfer of Wild-Type (+/+) BMMCs Reconstitutes LPS-Mediated Enhancement of Eosinophilic Airway Inflammation in W/W^v Mice. To further investigate the requirement of mast cells in enhanced eosinophilic inflammation induced by OVA plus LPS, wild-type mast cells were adoptively transferred into W/W^v mice. BMMCs were generated by culturing bone marrow cells with IL-3 for 4 weeks. A summary of infiltrating cells in the BAL fluid is presented in Fig. 2*A*, and representative photographic views of infiltrated cells (May–Giemsa staining) in each group are shown in Fig. 10, which is published as supporting information on the PNAS web site. The administration of +/+ BMMCs resulted in the dramatic eosinophilic infiltration in the BAL fluid of W/W^v mice immunized OVA and LPS when compared with mice not given wild-type (+/+) BMMCs (see Fig. 10*h*). No apparent effect was observed in the numbers of macrophages, neutrophils, and lymphocytes with the +/+ BMMC transfer.

Concurrently, histological analysis showed that the transfer of +/+ BMMCs as described above resulted in the dramatic increase in the levels of eosinophilic infiltration in the airway of W/W^v mice (Fig. 2*B*). There were also moderate increases in the numbers of total cells. Collectively, these results clearly indicate that mast cells play a critical role in LPS-mediated enhancement of airway eosinophilic inflammation.

TLR4 on Mast Cells Is Required for LPS-Mediated Enhancement of Eosinophilic Inflammation. The results thus far indicated that mast cells are critical for LPS-mediated enhancement of allergic airway eosinophilic inflammation. Because TLR4 is a known receptor for LPS (30), we next examined the involvement of TLR4 molecules on mast cells in the LPS-mediated enhancement of airway inflammation. BMMCs prepared from TLR4 KO mice showed a normal surface phenotype, e.g., the expression of c-*kit* and FcεRI (data not shown). Ten million BMMCs prepared from wild-type or TLR4 KO mice were transferred into W/W^v mice. As anticipated, the levels of eosinophilic infiltration were enhanced by the administration of wild-type (+/+), but not in the case of TLR4 KO, BMMCs (Fig. 2*C*; and see Fig. 11, which is published as supporting information on the PNAS web site). Also, LPS-mediated enhancement in the total numbers of infiltrating leukocytes was marginal in the TLR4 KO BMMC transfer group. It would appear that TLR4 on mast cells is crucial for LPS-mediated enhancement of eosinophilic inflammation.

To further investigate the involvement of TLR4 on mast cells, wild-type and TLR4 KO BMMCs were first treated with LPS (10 μg/ml) for 7 days *in vitro* and then transferred into W/W^v mice. No immunization was performed. Two days after the challenge with OVA, infiltrated cells in the BAL fluid were assessed. As shown in Fig. 2*D*, although the levels were modest, a significant increase in the number of eosinophils was detected with the administration of wild-type BMMCs pretreated with LPS. Representative photographic views of infiltrated cells (May–Giemsa staining) are shown in Fig. 12, which is published as supporting information on the

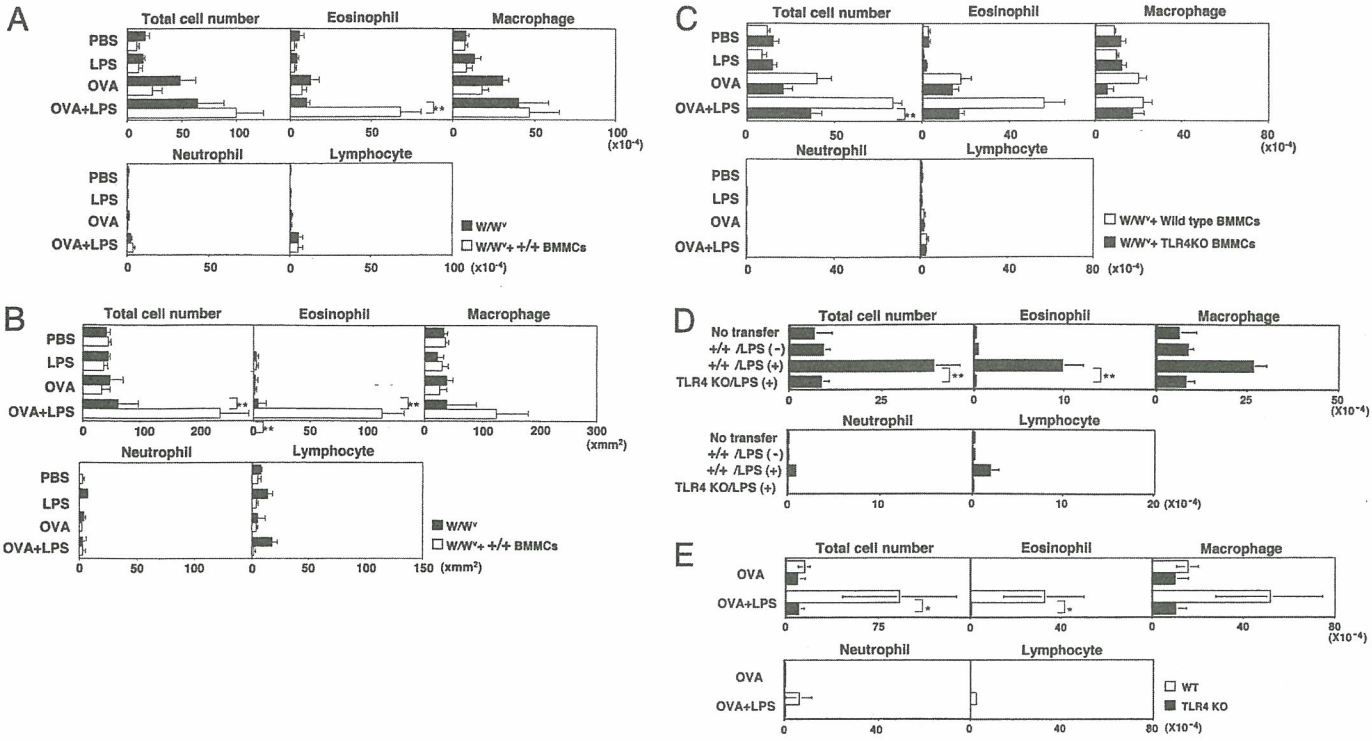

Fig. 2. TLR4 on mast cells is required for LPS-induced enhancement of eosinophilic inflammation. (*A*) BMMCs (1×10^7) were transferred intravenously 2 days before the initial OVA sensitization. The mean values, with standard deviation, of numbers of total cells and each cell type in the BAL fluid of W/W^v mice reconstituted with wild-type (+/+) BMMCs are shown. Ten mice were used in each group. **, <0.01 (Dunnett multiple comparisons test). (*B*) Histological analysis of the lung with H.E. and Luna staining. Mean values, with standard deviation, of infiltrated cells in 1 mm^2 are shown. Ten lung sections per mouse from three mice in each group were examined. **, <0.01 (Dunnett multiple comparisons test). (*C*) Infiltrated cells in BAL fluid of W/W^v mice reconstituted with wild-type (+/+) and TLR4 KO BMMCs are shown. Ten mice were used in each group. **, <0.01 (Dunnett multiple comparisons test). (*D*) Infiltrated cells in BAL fluid of W/W^v mice reconstituted with wild-type (+/+) and TLR4 KO BMMCs precultured with or without LPS (10 μg/ml) for 7 days are shown. No immunization was performed. Ten mice were used in each group. **, $P < 0.01$ (Student *t* test). (*E*) Wild-type and TLR4 KO mice were immunized and challenged, and infiltrated cells in the BAL fluid were assessed as in Fig. 1*A*. *, $P < 0.05$ (Student *t* test).

PNAS web site. Moreover, TLR4 KO mice were challenged directly with/without LPS and OVA to assess the LPS-mediated enhancement of airway inflammation, and no enhancing effect of LPS on the eosinophilic infiltration was observed in TLR4 KO mice (Fig. 2*E*; and see Fig. 13, which is published as supporting information on the PNAS web site). The LPS-induced increase in the number of other cell types, including macrophages and neutrophils, was modest, and no increase was seen in TLR4 KO mice.

Treatment with LPS Modulates Cytokine Production Profiles of Mast Cells. To analyze the molecular changes induced in mast cells after LPS treatment, BMMCs were cultured with or without LPS treatment (10 μg/ml) for 1 week *in vitro*. The expression levels of FcεRI, c-*kit*, I-K, CD54, and RIPA/B were similar between wild-type and TLR4 KO BMMCs before and after LPS treatment (data not shown). The LPS-treated BMMCs were then restimulated with phorbol 12-myristate 13-acetate (PMA) plus ionomycin, and the ability to produce various cytokines (IL-5, -13, -6, and -4 and TNF-α) was assessed by ELISA. The levels of IL-5 and -13 were substantially increased after LPS treatment, whereas the production of IL-6 and TNF-α was only slightly increased (Fig. 3*A*). IL-4 was not detected with or without LPS treatment (data not shown).

Next, we assessed the mRNA expression of IL-4, -5, and -13 and Eotaxin-2 after IgE/Ag stimulation in wild-type and TLR4 KO BMMCs cultured with LPS. The mRNA expression of IL-4, -5, and -13 and Eotaxin-2 was increased dramatically for all of these cytokines in wild-type BMMCs. In the case of TLR4 KO BMMCs, however, the increase was seen in the case of IL-4 and -13 but not in the case of IL-5 and Eotaxin-2 (Fig. 3*B*). More specifically, the induction in IL-5 was barely detectable, indicating that the Ag/IgE-induced expression of IL-5 was most sensitive to the effect of LPS/TLR4-mediated modification of BMMC function.

To assess more directly whether LPS/TLR4-mediated signaling synergizes with IgE/Ag-dependent responses in BMMCs, BMMCs were stimulated with combinations of LPS and IgE/Ag *in vitro*. As shown in Fig. 3*C*, clear synergistic effects were observed in the expression of IL-5 and -13 and some effect on Eotaxin-2 but much less in the case of IL-4.

LPS Treatment Induces NF-κB Activation and Increases Expression of GATA1 and -2 in BMMCs. Because NF-κB is activated through TLR4 after LPS ligation (18), we wanted to test whether LPS treatment induces NF-κB activation in mast cells. A gel-shift assay for NF-κB was performed with BMMCs treated with LPS. A significant activation of NF-κB was detected in wild-type BMMCs but not in TLR4 KO BMMCs (Fig. 3*D Left*). In an AP-1 gel-shift assay, a modest increase was detected after LPS treatment, but no difference was observed between wild-type and TLR4 KO groups (Fig. 3*D Right*).

Although GATA3 is reported to be a downstream target of NF-κB activation (31) and is critical for chromatin remodeling of the Th2 cytokine gene loci (32–34) and transcription of the *IL-5* and *IL-13* genes in Th2 cells (35–37), GATA3 is not expressed in BMMCs (7). In contrast, GATA1 and -2 play a key role in mast-cell differentiation (38, 39). We examined the levels of protein expression of GATA1 and -2 in BMMCs treated with LPS. As shown in Fig. 3*E*, the levels of GATA1 and -2, but not -3, were substantially increased in the BMMCs after LPS treatment for 3 days. The

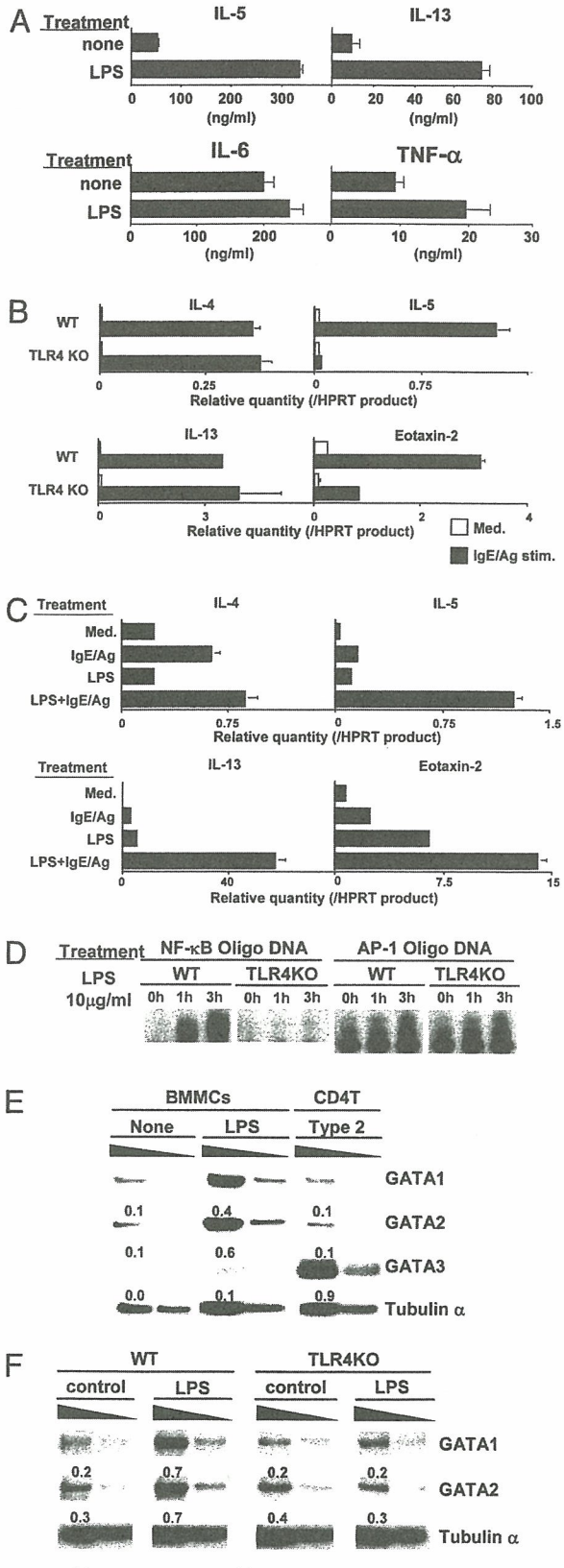

Fig. 3. Cytokine-expression profiles and NF-κB activation in BMMCs treated with LPS. (*A*) BMMCs were cultured with LPS for 1 week. Then, BMMCs were restimulated with PMA (10 ng/ml) and ionomycin (1 μM) for 24 h to assess the production of IL-5, -13, and -6 and TNF-α by ELISA. Four experiments with individual BMMC preparations were performed, and similar results were obtained. (*B*) Wild-type (+/+) and TLR4 KO BMMCs were cultured with LPS for 1 week and then stimulated with IgE/Ag. Transcriptional levels of IL-4, -5, and -13 and Eotaxin-2 were determined by real-time RT-PCR analysis. Two independent experiments were performed, and similar results were obtained. (*C*) Wild-type BMMCs were stimulated with combinations of LPS and IgE/Ag. Transcriptional levels of IL-4, -5, and -13 and Eotaxin-2 were determined by real-time RT-PCR analysis. Two independent experiments were performed, and similar results were obtained. (*D*) EMSAs for NF-κB and AP-1. Nuclear extracts of wild-type and TLR4 KO BMMCs treated with LPS for 1 and 3 h were subjected to EMSAs with NF-κB and AP-1 probes. Two independent experiments were performed, and similar results were obtained. (*E*) The levels of protein expression of GATA1 and -2 in LPS-stimulated BMMCs. BMMCs treated with LPS for 3 days and CD4 T cells cultured under Th2-skewed conditions for 3 days were prepared. Nuclear extracts were used for immunoblotting with specific mAbs specific for GATA1, -2, and -3. Arbitrary densitometric units normalized with the band intensity of tubulin α are shown under each band. Three experiments were performed, and similar results were obtained. (*F*) GATA1 and -2 expression in LPS-treated BMMCs from wild-type and TLR4 KO mice. Two experiments were performed, and similar results were obtained.

LPS-induced increase in the levels of GATA1 and -2 protein was not detected in TLR4 KO BMMCs (Fig. 3*F*), but increases were detected in STAT6 KO BMMCs (data not shown). The increase in GATA1 and -2 protein was also observed after 7-day cultures (data not shown). Thus, TLR4-mediated signaling is critical for GATA1 and -2 up-regulation in BMMCs upon LPS treatment.

GATA1 Controls the Expression of Th2 Cytokines in Mast Cells. Finally, we studied whether GATA1 and -2 can play a functional role in transcription of IL-5, -13, and -4 in mast cells. We used a MC9 mast-cell line for a reporter gene assay. The introduction of GATA1, but not -2 or -3, into MC9 cells resulted in substantial induction of the reporter activities of IL-4 and -5 promoters (Fig. 4*A*). When GATA1 was introduced by retrovirus into MC9 cells, the mRNA expression of IL-4, -5, and -13, but not of Eotaxin-2, was increased significantly (Fig. 4*B*). The increase in Th2 cytokine mRNA was not observed with GATA2 overexpression. Furthermore, we tested whether the inhibition of GATA1 expression in BMMCs would result in decreased expression of Th2 cytokines. BMMCs cultured with LPS were transfected with small interfering (si)RNA specific for GATA1 during the treatment with LPS stimulated with PMA plus ionomycin, and then the transcriptional levels of Th2 cytokines were determined by quantitative PCR. As expected, the mRNA levels of IL-4, -5, and -13 were all decreased significantly (Fig. 4*C*). These results suggest that GATA1 controls the expression of Th2 cytokines in mast cells, such as MC9 and BMMCs, with LPS stimulation.

Discussion

The results presented here indicate that mast cells and their TLR4 molecules are crucial for LPS-mediated enhancement of allergic airway eosinophilic inflammation. After LPS treatment, BMMCs acquired an increased ability to produce Th2 cytokines, such as IL-5 and -13. Clear synergistic effects in the expression of IL-5 and -13 were detected in LPS-treated BMMCs after costimulation with LPS and IgE/Ag. GATA1 appeared to be important for the transcription of Th2 cytokines in mast cells. These findings suggest that LPS-induced TLR4 signaling modulates mast-cell function and regulates allergic airway inflammation *in vivo*.

Dendritic cells (DCs) are well recognized to play a central role in inflammatory reactions elicited by LPS (16). When DCs are activated by LPS through TLR4, they become mature and acquire an increased ability to prime T cells (40). In particular, mature DCs produce increased levels of IL-1 and -12 and TNF-α that lead to the promotion of Th1-skewed responses (41). However, it is also well recognized in humans that LPS is a risk factor for asthma (42, 43). In some mouse models, LPS was reported to elicit airway inflammation (14, 22, 44). To investigate the molecular basis underlying the LPS-induced mast-cell activation and regulation of allergic eosinophilic airway inflammation, we used an experimental model with a low-dose LPS administration, in which Th2-dependent

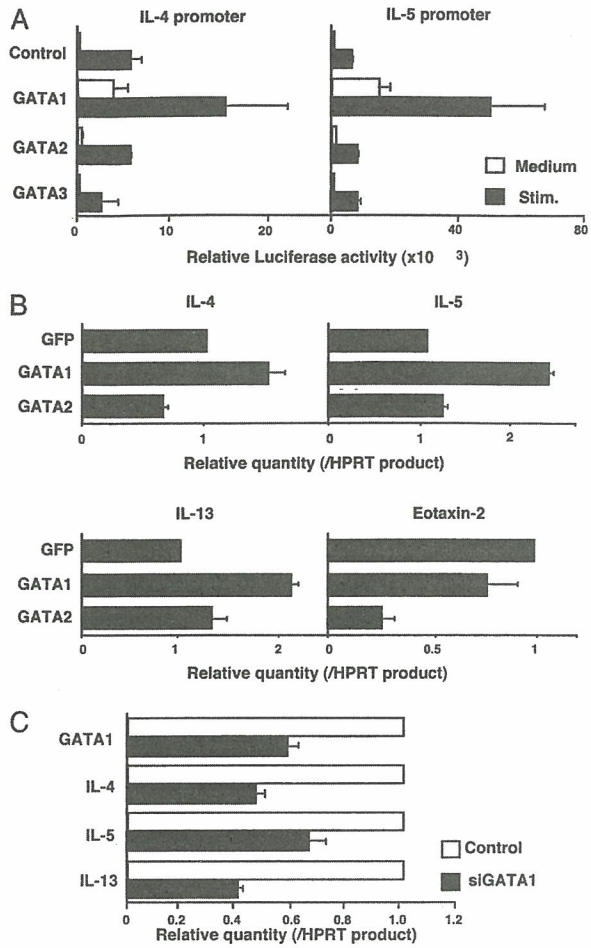

Fig. 4. GATA1 controls the expression of Th2 cytokines in mast cells. (*A*) A reporter gene assay was done with IL-4 and -5 promoters by using the MC9 mast-cell line. The mean values, with standard deviation, of relative luciferase activity of four different experiments are shown. (*B*) MC9 cells were infected with retrovirus encoding GATA1 or -2 bicistronically with EGFP. GFP-positive infected cells were enriched by cell-sorting and stimulated with PMA (25 ng/ml) plus ionomycin (500 nM) for 18 h. Quantitative real-time RT-PCR was performed. (*C*) Inhibition of Th2 cytokine expression by the introduction of siRNA for GATA1. BMMCs were transfected with siRNA specific for GATA1. Two days after transfection, the cells were stimulated with PMA plus ionomycin, and transcriptional levels of GATA1 and Th2 cytokines were determined by quantitative RT-PCR. Two experiments were done with similar results.

eosinophilic airway inflammation is selectively induced (14). As for a mechanism, Eisenbarth *et al.* (14) suggested the importance of LPS-induced DC activation for the induction of eosinophilic airway inflammation. From the studies presented here, we propose a different mechanism, whereby mast cells, another innate immunity cell type, play a crucial role for regulating eosinophilic airway inflammation. LPS-induced mast-cell activation and modulation with increased production of Th2 cytokines, such as IL-5 and -13, appear to control the severity of eosinophilic airway inflammation.

It is known that IL-5 and -13 play crucial roles in the induction and the severity of eosinophilic airway inflammation in the lung (45). The levels of Th2 cytokines, such as IL-5 and -13, produced by mast cells were increased dramatically after LPS treatment (Fig. 3*A*). We detected decreased levels of IL-4, -5, and -13 and Eotaxin-2 in BAL fluid cells from mast-cell-deficient W/W^v mice as compared with +/+ mice (Fig. 6). The IgE/Ag-induced IL-5 expression in BMMCs was minimal in TLR4 KO BMMCs (Fig. 3*B*). Moreover, obvious synergistic effects in the expression of IL-5 and -13 were detected in LPS-treated BMMCs after costimulation with LPS and IgE/Ag (Fig. 3*C*). Thus, although it is difficult to determine which Th2 cytokines produced by mast cells are most important for LPS-mediated enhancement of allergic eosinophilic inflammation, a direct effect of IL-5 in the activation and migration of eosinophils in the lung appears to be critical. Because BMMCs also produce increased TNF-α ($\approx$2-fold) after LPS treatment (Fig. 3*A*), it is conceivable that TNF-α produced from activated mast cells may also induce DC maturation and regulate eosinophilic airway inflammation. In addition, Eotaxin-2 expression induced by IgE/Ag stimulation in BMMCs (Fig. 3 *B* and *C*) may also contribute to the inflammation by increasing eosinophil migration into the lung.

After *in vitro* LPS stimulation for a short period (<16 h), Supajatura V. *et al.* (21) reported that BMMCs produced TNF-α, IL-1β, -6, and -13 but not IL-4 or -5. Similarly Matsuda *et al.* (22) reported that LPS induced the production of IL-5, -10, and -13, but not of IL-4, in BMMCs. The levels of cytokine production detected in those studies were much lower than those detected in this study (Fig. 3*A*), due, perhaps, to the different methods of LPS treatment. In our studies, to assess the changes in the ability to produce cytokines in BMMCs, the cells were treated with LPS for 1 week (Fig. 3*A*). We observed some increase in acetylation of histone H3/K9 at the Th2 cytokine gene loci, suggesting the occurrence of chromatin remodeling (M.Y. and T.N., unpublished observation). Although we do not know whether the LPS treatment induced a true "maturation" of BMMCs, it is clear that BMMCs acquired an ability to produce increased amounts of Th2 cytokines after LPS treatment for 1 week, reminiscent of the maturation process of DCs after LPS stimulation (40).

It has been reported that airway hyperreactivity to methacholine is modulated by the administration of high-dose LPS in rats (44) and mice (46). In the current experimental system, where a mild OVA sensitization protocol was used, we did not observe clear induction of airway hyperreactivity, and treatment with LPS/OVA did not change this situation significantly (M.Y. and T.N., unpublished observation). Further investigation will be needed to clarify the effect of LPS and the contribution of mast cells in the development of airway hyperreactivity.

In summary, in a mouse allergic asthma model, we found that mast cells play a crucial role for LPS-mediated enhancement of eosinophilic airway inflammation. Moreover, TLR4 molecules on mast cells were critical for LPS-induced mast-cell activation and functional modulation. Thus, a search for specific inhibitors acting on the TLR4-mediated signal transduction pathway could lead to an approach for the treatment of inflammation in patients with bronchial asthma, particularly during respiratory infection.

Materials and Methods

Animals. C57BL/6, WBB6F1 W/W^v mice (47) with (WBxC57BL6)F1 background and WBB6F1 +/+ were purchased from Japan SLC (Shizuoka, Japan). STAT6-deficient and TLR4-deficient (TLR4 KO) mice backcrossed eight times with C57BL/6 mice were kindly provided by Dr. Shizuo Akira (Osaka University) (30, 48). All mice used in this study were maintained under specific-pathogen-free conditions. Animal care was in accordance with the guidelines of Chiba University.

Cell Cultures. BMMCs were generated as described in ref. 29.

Immunization and Challenge. Female mice (6–7 weeks old) were anesthetized with ketamine hydrochloride, xylazine, and flunitrazepam i.p. and sensitized intranasally with 10 μg of OVA [Grade V; Sigma Aldrich, LPS contamination <0.5 ng; measured by limulus amebocyte assay (Bio-Whittaker)] and 1 μg of LPS (*Escherichia coli* O55:B5, List Biological Laboratories, Campbell, CA) in 35 μl of PBS on days 0, 1, and 2. The sensitized mice were challenged on days 14, 15, 18, and 19 intranasally with 25 μg of OVA in 35 μl of PBS under anesthesia as described in ref. 14.

Collection and Analysis of BAL Fluid. Two days after the last challenge with OVA, BAL was prepared as described in refs. 28 and 29. One-hundred thousand viable BAL cells were cytocentrifuged onto slides by using a Cytospin 3 (Shandon, Pittsburgh) and stained with May–Grunwald–Giemsa solution (Merck) as described in ref. 9. Two hundred leukocytes were counted in each slide. Cell types were identified based on morphological criteria.

Lung Histology. On day 20, 1 day after the last OVA challenge, mice were killed by CO_2 asphyxiation, and the lungs were infused with 10% (vol/vol) formalin in PBS for fixation and then subjected to H.E., Luna, or Masson–trichrome staining as described in refs. 28 and 29.

Treatment of BMMCs with LPS *in Vitro*. BMMCs were cultured with or without LPS (10 μg/ml) for 7 days. The LPS-stimulated BMMCs were activated with PMA (10 ng/ml) and ionomycin (1 μM), or with IgE/Ag (anti-DNP IgE and DNP) as described in ref. 49. In the experiments addressing a direct synergistic effect between LPS stimulation and IgE/Ag stimulation, BMMCs were stimulated with a combination of LPS (10 μg/ml) and IgE/Ag *in vitro* for 24 h. The production of cytokines was assessed by ELISA as described in ref. 50. For transfer experiments, BMMCs (1×10^7) were transferred into W/W^v mice 2 days before the first immunization. In some experiments, BMMCs were pretreated with LPS (10 μg/ml) for 7 days before transfer, and no LPS was used for *in vivo* priming.

RT-PCR. Quantitative RT-PCR was performed by using Gene Expression assay (Applied Biosystems) and ABI prism 2000 as described in ref. 34. Hypoxanthine phosphoribosyltransferase was used for a control. The specific primers for detection of cytokines were described in ref. 34. Primer pairs for Eotaxin-2 are tagcctgcgcgtgttgcatcttcc-3′ and 5′-taaacctcggtgctattgccacgg.

Immunoblot Analysis. Immunoblot analysis for GATA1, -2 and -3 was performed as described in ref. 34. Anti-GATA1 (N1), anti-GATA2 (CG2–96) and anti-GATA3 (HG3–31) (all from Santa Cruz Biotechnology) antibodies were used.

Luciferase Reporter Assay. Luciferase assay was performed by using Dual Luciferase Reporter instructions as described in ref. 32. A single copy of an IL-4 promoter (−766 bp) and IL-5 promoter (−1,200 bp) in the luciferase reporter plasmid pGL2 Basic (Promega) and MC9 (a mast-cell line expressing some levels of GATA1 and -2 but not GATA3) cells were used.

EMSA EMSAs were performed by using Gel Shift Assay Systems (Promega) as described in ref. 51.

siRNA. Introduction of siRNA into BMMCs was performed as described in ref. 52. Predesigned siRNA for GATA1 was purchased from Ambion (#16704). In brief, 2 μl of TransIT-TKO transfection reagent (Mirus, Madison, WI) was diluted in 50 μl of serum-free/antibiotic-free RPMI medium 1640. Ten minutes later, 1 μl of 40 μM siRNA was added to the diluted transfection reagent and incubated for 30 min with gentle agitation. The siRNA solution was added to BMMC cultures containing 5×10^5 cells in 500 μl of medium per well in a 24-well plate. Two days after transfection, expression levels of GATA1 and IL-4, -5, and -13 mRNA were assessed by quantitative RT-PCR.

We thank Drs. Ralph T. Kubo and Kiyoshi Takeda for helpful comments and constructive criticism in the preparation of the manuscript and Ms. Kaoru Sugaya, Satoko Norikane, and Hikari Asou for excellent technical assistance. This work was supported by Ministry of Education, Culture, Sports, Science and Technology (Japan) Grants 17016010 and 17047007, Grants-in-Aid for Scientific Research in Priority Areas, Scientific Research B 17390139 and Scientific Research C 16616003; Grants-in-Aid for Young Scientists 17790317 and 17790318; and Special Coordination Funds for Promoting Science and Technology, the Ministry of Health, Labor and Welfare (Japan), the Program for Promotion of Fundamental Studies in Health Sciences of the National Institute of Biomedical Innovation (Japan), the Japan Health Science Foundation, the Kanae Foundation, the Uehara Memorial Foundation, and the Mochida Foundation.

1. Metcalfe, D. D., Kaliner, M. & Donlon, M. A. (1981) *Crit. Rev. Immunol.* **3,** 23–74.
2. Schwartz, L. B. & Austen, K. F. (1984) *Prog. Allergy* **34,** 271–321.
3. Galli, S. J. (1993) *N. Engl. J. Med.* **328,** 257–265.
4. Boyce, J. A. (2003) *Prostaglandins Leukotrienes Essent. Fatty Acids* **69,** 195–205.
5. Brightling, C. E., Bradding, P., Pavord, I. D. & Wardlaw, A. J. (2003) *Clin. Exp. Allergy* **33,** 550–556.
6. Drazen, J. M., Arm, J. P. & Austen, K. F. (1996) *J. Exp. Med.* **183,** 1–5.
7. Weiss, D. L. & Brown, M. A. (2001) *Immunol. Rev.* **179,** 35–47.
8. Hamelmann, E. & Gelfand, E. W. (2001) *Immunol. Rev.* **179,** 182–191.
9. Foster, P. S., Hogan, S. P., Ramsay, A. J., Matthaei, K. I. & Young, I. G. (1996) *J. Exp. Med.* **183,** 195–201.
10. Gern, J. E. (2000) *J. Allergy Clin. Immunol.* **105,** S497–S502.
11. Liu, A. H. (2002) *J. Allergy Clin. Immunol.* **109,** 379–392.
12. Schwartz, D. A. (2001) *Am. J. Respir. Crit. Care Med.* **163,** 305–306.
13. Braun-Fahrlander, C., Riedler, J., Herz, U., Eder, W., Waser, M., Grize, L., Maisch, S., Carr, D., Gerlach, F., Bufe, A., *et al.* (2002) *N. Engl. J. Med.* **347,** 869–877.
14. Eisenbarth, S. C., Piggott, D. A., Huleatt, J. W., Visintin, I., Herrick, C. A. & Bottomly, K. (2002) *J. Exp. Med.* **196,** 1645–1651.
15. Janeway, C. A., Jr., & Medzhitov, R. (2002) *Annu. Rev. Immunol.* **20,** 197–216.
16. Akira, S., Takeda, K. & Kaisho, T. (2001) *Nat. Immunol.* **2,** 675–680.
17. Iwasaki, A. & Medzhitov, R. (2004) *Nat. Immunol.* **5,** 987–995.
18. Takeda, K., Kaisho, T. & Akira, S. (2003) *Annu. Rev. Immunol.* **21,** 335–376.
19. Medzhitov, R. (2001) *Nat. Rev. Immunol.* **1,** 135–145.
20. McCurdy, J. D., Lin, T. J. & Marshall, J. S. (2001) *J. Leukoc. Biol.* **70,** 977–984.
21. Supajatura, V., Ushio, H., Nakao, A., Akira, S., Okumura, K., Ra, C. & Ogawa, H. (2002) *J. Clin. Invest.* **109,** 1351–1359.
22. Masuda, A., Yoshikai, Y., Aiba, K. & Matsuguchi, T. (2002) *J. Immunol.* **169,** 3801–3810.
23. Okumura, S., Kashiwakura, J., Tomita, H., Matsumoto, K., Nakajima, T., Saito, H. & Okayama, Y. (2003) *Blood* **102,** 2547–2554.
24. Malaviya, R., Ikeda, T., Ross, E. & Abraham, S. N. (1996) *Nature* **381,** 77–80.
25. Echtenacher, B., Mannel, D. N. & Hultner, L. (1996) *Nature* **381,** 75–77.
26. Supajatura, V., Ushio, H., Nakao, A., Okumura, K., Ra, C. & Ogawa, H. (2001) *J. Immunol.* **167,** 2250–2256.
27. McLachlan, J. B., Hart, J. P., Pizzo, S. V., Shelburne, C. P., Staats, H. F., Gunn, M. D. & Abraham, S. N. (2003) *Nat. Immunol.* **4,** 1199–1205.
28. Shibata, Y., Kamata, T., Kimura, M., Yamashita, M., Wang, C. R., Murata, K., Miyazaki, M., Taniguchi, M., Watanabe, N. & Nakayama, T. (2002) *J. Immunol.* **169,** 2134–2140.
29. Kamata, T., Yamashita, M., Kimura, M., Murata, K., Inami, M., Shimizu, C., Sugaya, K., Wang, C. R., Taniguchi, M. & Nakayama, T. (2003) *J. Clin. Invest.* **111,** 109–119.
30. Hoshino, K., Takeuchi, O., Kawai, T., Sanjo, H., Ogawa, T., Takeda, Y., Takeda, K. & Akira, S. (1999) *J. Immunol.* **162,** 3749–3752.
31. Das, J., Chen, C. H., Yang, L., Cohn, L., Ray, P. & Ray, A. (2001) *Nat. Immunol.* **2,** 45–50.
32. Yamashita, M., Ukai-Tadenuma, M., Kimura, M., Omori, M., Inami, M., Taniguchi, M. & Nakayama, T. (2002) *J. Biol. Chem.* **277,** 42399–42408.
33. Inami, M., Yamashita, M., Tenda, Y., Hasegawa, A., Kimura, M., Hashimoto, K., Seki, N., Taniguchi, M. & Nakayama, T. (2004) *J. Biol. Chem.* **279,** 23123–23133.
34. Omori, M., Yamashita, M., Inami, M., Ukai-Tadenuma, M., Kimura, M., Nigo, Y., Hosokawa, H., Hasegawa, A., Taniguchi, M. & Nakayama, T. (2003) *Immunity* **19,** 281–294.
35. Lee, H. J., O'Garra, A., Arai, K. & Arai, N. (1998) *J. Immunol.* **160,** 2343–2352.
36. Zhang, D. H., Yang, L. & Ray, A. (1998) *J. Immunol.* **161,** 3817–3821.
37. Schwenger, G. T., Fournier, R., Kok, C. C., Mordvinov, V. A., Yeoman, D. & Sanderson, C. J. (2001) *J. Biol. Chem.* **276,** 48502–48509.
38. Harigae, H., Takahashi, S., Suwabe, N., Ohtsu, H., Gu, L., Yang, Z., Tsai, F. Y., Kitamura, Y., Engel, J. D. & Yamamoto, M. (1998) *Genes Cells* **3,** 39–50.
39. Migliaccio, A. R., Rana, R. A., Sanchez, M., Lorenzini, R., Centurione, L., Bianchi, L., Vannucchi, A. M., Migliaccio, G. & Orkin, S. H. (2003) *J. Exp. Med.* **197,** 281–296.
40. Banchereau, J. & Steinman, R. M. (1998) *Nature* **392,** 245–252.
41. Schnare, M., Barton, G. M., Holt, A. C., Takeda, K., Akira, S. & Medzhitov, R. (2001) *Nat. Immunol.* **2,** 947–950.
42. Rizzo, M. C., Naspitz, C. K., Fernandez-Caldas, E., Lockey, R. F., Mimica, I. & Sole, D. (1997) *Pediatr. Allergy Immunol.* **8,** 121–126.
43. Michel, O., Ginanni, R., Duchateau, J., Vertongen, F., Le Bon, B. & Sergysels, R. (1991) *Clin. Exp. Allergy* **21,** 441–448.
44. Tulic, M. K., Wale, J. L., Holt, P. G. & Sly, P. D. (2000) *Am. J. Respir. Cell Mol. Biol.* **22,** 604–612.
45. Herrick, C. A. & Bottomly, K. (2003) *Nat. Rev. Immunol.* **3,** 405–412.
46. Lefort, J., Singer, M., Leduc, D., Renesto, P., Nahori, M. A., Huerre, M., Creminon, C., Chignard, M. & Vargaftig, B. B. (1998) *J. Immunol.* **161,** 474–480.
47. Kitamura, Y., Go, S. & Hatanaka, K. (1978) *Blood* **52,** 447–452.
48. Takeda, K., Tanaka, T., Shi, W., Matsumoto, M., Minami, M., Kashiwamura, S., Nakanishi, K., Yoshida, N., Kishimoto, T. & Akira, S. (1996) *Nature* **380,** 627–630.
49. Yamasaki, S., Ishikawa, E., Kohno, M. & Saito, T. (2004) *Blood* **103,** 3093–3101.
50. Kimura, M., Koseki, Y., Yamashita, M., Watanabe, N., Shimizu, C., Katsumoto, T., Kitamura, T., Taniguchi, M., Koseki, H. & Nakayama, T. (2001) *Immunity* **15,** 275–287.
51. Kimura, M. Y., Hosokawa, H., Yamashita, M., Hasegawa, A., Iwamura, C., Watarai, H., Taniguchi, M., Takagi, T., Ishii, S. & Nakayama, T. (2005) *J. Exp. Med.* **201,** 397–408.
52. Yamashita, M., Shinnakasu, R., Asou, H., Kimura, M., Hasegawa, A., Hashimoto, K., Hatano, N., Ogata, M. & Nakayama, T. (2005) *J. Biol. Chem.* **280,** 29409–29419.

Impaired GATA3-Dependent Chromatin Remodeling and Th2 Cell Differentiation Leading to Attenuated Allergic Airway Inflammation in Aging Mice[1]

Akihiro Hasegawa,* Takako Miki,* Hiroyuki Hosokawa,* Mohammad B. Hossain,* Chiori Shimizu,* Kahoko Hashimoto,† Motoko Y. Kimura,* Masakatsu Yamashita,* and Toshinori Nakayama[2]*

Age-related changes in lymphocytes are most prominent in the T cell compartment. There have been substantial numbers of reports on T cell function in aged mice and humans, such as on the production of Th1 and Th2 cytokines, but the results show considerable variation and contradictions. In the present study, we used 8- to 12-mo-old aging mice and a well-established in vitro Th1/Th2 cell differentiation culture system to identify molecular defects in Th1/Th2 cell differentiation that can be detected in the relatively early stages of aging. The capability to differentiate into Th2 cells is reduced in aging mouse $CD4^+$ T cells. Decreased activation of the ERK MAPK cascade upon TCR stimulation, but normal intracellular-free calcium ion concentration mobilization and normal IL-4-induced STAT6 activation were observed in aging mouse $CD4^+$ T cells. In addition, reduced expression of GATA3 was detected in developing Th2 cells. Chromatin remodeling of the Th2 cytokine gene locus was found to be impaired. Th2-dependent allergic airway inflammation was milder in aging mice compared with in young adult mice. These results suggest that the levels of Th2 cell differentiation and resulting Th2-dependent immune responses, including allergic airway inflammation, decline during aging through defects in the activation of the ERK MAPK cascade, expression of GATA3 protein and GATA3-dependent chromatin remodeling of the Th2 cytokine gene locus. In the present study, we provide the first evidence indicating that a chromatin-remodeling event in T cells is impaired by aging. *The Journal of Immunology,* **2006, 176: 2546–2554.**

The $CD4^+$ T cells consist of two distinct Th cell subpopulations, Th1 and Th2 cells (1). Th1 cells produce IFN-γ and are involved in cell-mediated immunity against intracellular pathogens. Th2 cells produce IL-4, IL-5, and IL-13 and control humoral immunity and allergic reactions. Naive $CD4^+$ T cells differentiate into Th1 cells following recognition of Ags in the presence of IL-12, whereas IL-4 drives differentiation into Th2 cells (2–4). In addition to the cytokines mentioned above, TCR stimulation by Ags is also indispensable for both Th1and Th2 cell differentiation. We reported that the efficient TCR-mediated activation of $p56^{lck}$, calcineurin, and the Ras-ERK MAPK signaling cascade is required for Th2 cell differentiation (5–7). Several transcription factors that control Th1/Th2 cell differentiation have been identified (8, 9). Among them, GATA3 appears to be a master transcription factor for Th2 cell differentiation (10–13) and Th2 cell maintenance (14, 15). Recently, we reported that the activation of the ERK MAPK cascade inhibits the ubiquitin-dependent degradation of GATA3 in developing Th2 cells and facilitates GATA3-dependent chromatin remodeling of the Th2 cytokine gene locus (16).

In the elderly, there is an increase in the frequency and severity of infectious diseases (17–19). Age-related changes in the immune system occur mainly in the T cell compartment (20–22). There may be related to a decrease in the ability of T cells to proliferate, and are associated with a reduction in IL-2 production (23) and reduced IL-2R expression (24–26). Various alterations in signaling have been described in comparison with young T cells. $CD4^+$ T cells from old mice show defects in TCR signal transduction that include diminished TCR-ζ phosphorylation, decreased elevation of intracellular Ca^+, and diminished activation of the MEK/ERK pathway (20, 27, 28). In contrast, aging does not affect Zap70-TCR-ζ association (29).

T cells in the elderly are often characterized by a shift from naive to memory phenotypes (30, 31). The production of the type 1 cytokine IFN-γ has been reported to be increased (32–34) or decreased (35–37) in aged mice and humans. Also, the production of type 2 cytokines such as IL-4 and IL-5 has been reported to be increased (38, 39) or decreased (33, 35) in vitro. These controversial observations on cytokine production may be a result of variations among the species or strains used in experiments, housing conditions or experimental culture systems. At present, age-related molecular defects in developing Th1/Th2 cells that control Th1/Th2 cytokine gene chromatin remodeling have not been formally investigated. In addition, it is not well clarified whether the severity of Th2-dependent allergic responses, such as allergic asthma, is modulated by aging.

*Department of Immunology, Graduate School of Medicine, Chiba University, Chiba, Japan; and †Department of Life and Environmental Sciences and High Technology Research Center, Chiba Institute of Technology, Chiba, Japan

Received for publication August 19, 2005. Accepted for publication November 30, 2005.

The costs of publication of this article were defrayed in part by the payment of page charges. This article must therefore be hereby marked *advertisement* in accordance with 18 U.S.C. Section 1734 solely to indicate this fact.

[1] This work was supported by grants from the Ministry of Education, Culture, Sports, Science, and Technology (Japan) (Grants-in-Aid for Scientific Research, Priority Areas Research 17016010 and 17047007; Scientific Research B 17390139; Scientific Research C 16616003; Young Scientists 17790317 and 17790318, and Special Coordination Funds for Promoting Science and Technology), the Ministry of Health, Labor, and Welfare (Japan), the Program for Promotion of Fundamental Studies in Health Science of the National Institute of Biomedical Innovation, the Japan Health Science Foundation, Uehara Memorial Foundation, Kanae Foundation, and the Mochida Memorial Foundation.

[2] Address correspondence and reprint request to Dr. Toshinori Nakayama, Department of Immunology, Graduate School of Medicine, Chiba University, 1-8-1 Inohana, Chuo-ku, Chiba 260-8670, Japan. E-mail address: tnakayama@faculty.chiba-u.jp

0022-1767/06/$02.00

In the present study, we demonstrate that Th2 cell differentiation and Th2-dependent immune responses in vivo, including OVA-induced airway inflammation, are attenuated in aging mice. We detected several molecular defects in aging mouse $CD4^+$ T cells that may account for the attenuated Th2 responses, i.e., 1) reduced activation of the ERK MAPK cascade upon TCR stimulation, 2) decreased GATA3 expression in developing Th2 cells, and 3) impaired chromatin remodeling of the Th2 cytokine gene locus.

Materials and Methods

Mice

C57BL/6 and BALB/c were purchased from Charles River Laboratories. All young adult (5–6 wk) and aging (8–12 mo) mice including OVA-specific TCR$\alpha\beta$ transgenic (DO.11.10 Tg) mice (40) used in this study were maintained under specific-pathogen-free conditions. Animal care was in accordance with the guidelines of Chiba University.

Immunofluorescent staining and flow cytometric analysis

In general, 1 million cells were incubated on ice for 30 min with the appropriate staining reagents, according to a standard method (41). The reagents used in this study, anti-CD4-PE (RM4-1-PE), anti-CD4-FITC (RM4-1-FITC), anti-CD44-PE, anti-IL-4Rα Ab, anti-CD25-FITC, and anti-CD69-FITC, were purchased from BD Pharmingen. Anti-rat Ig-FITC was purchased from CAPPEL. Anti-TCRβ-FITC (H57-FITC), anti-TCRβ-biotin, and anti-CD3-FITC (2C11-FITC) were prepared in our laboratory. Flow cytometric analysis was performed on a FACSCalibur (BD Biosciences), and the results were analyzed with CellQuest software (BD Biosciences). Intracellular staining of IL-4 and IFN-γ was performed as described previously (6). FITC- or allophycocyanin-conjugated anti-IFN-γ Ab (XMG1.2; BD Pharmingen) and PE- or allophycocyanin-conjugated anti-IL-4 Ab (11B11; BD Pharmingen) were used for detection.

Cell purification

Splenic $CD4^+$ T cells were stained with anti-CD4-FITC and then purified using anti-FITC magnetic beads (Miltenyi Biotec) and an AutoMACS sorter (Miltenyi Biotec), yielding a purity of >98%. In some experiments, spleen cells were stained with anti-CD4 and anti-CD44, and naive $CD4^+CD44^{low}$ T cells were sorted by a FACSVantage (BD Biosciences) and used as responder T cells as described previously (42).

Proliferation assay

Splenic $CD4^+$ T cells (2×10^5) prepared by the AutoMACS sorter were stimulated in 200-μl cultures for 40 h with immobilized anti-TCRβ mAb (H57-597). [^{3}H]Thymidine (37 kBq/well) was added to the stimulation culture for the last 16 h, and the incorporated radioactivity was measured on a beta plate (6).

Analysis of the efficiency of cell division

Splenic $CD4^+$ T cells purified by the AutoMACS sorter were labeled with CFSE (Molecular Probes) as described previously (42).

Measurement of intracellular-free calcium ion concentration ($[Ca^{2+}]_i$)[3]

Splenic $CD4^+$ T cells purified by the AutoMACS sorter were loaded with Indo-1 (Indo-1 AM; Molecular Probes) in the presence of F127 (41). After washing, the cells were incubated with anti-CD4-FITC and anti-TCRβ-biotin on ice. The stained cells were washed and subjected to Ca analysis on a FACSVantage (BD Biosciences). TCR was cross-linked with avidin, the $[Ca^{2+}]_i$ was monitored for 512 s, and the results were analyzed with CellQuest software (BD Biosciences).

In vitro Th1/Th2 cell differentiation cultures

DO11.10 Tg $CD44^{low}CD4^+$ T cells (1.5×10^4) purified by cell sorting were stimulated with antigenic OVA peptide (OVA; 323–339, 10 μM) and irradiated (3000 rad) BALB/c APCs (1×10^5) in the presence of exogenous IL-4 or IL-12 as described previously (6).

[3] Abbreviations used in this paper: $[Ca^{2+}]_i$, free calcium ion concentration; ChIP, chromatin immunoprecipitation; BAL, bronchioalveolar lavage.

ELISA for the measurement of cytokine concentration

The productions of IL-2, IL-4, IL-5, IL-13, and IFN-γ were measured by ELISA as described previously (43).

RT-PCR analysis

The quantitative RT-PCR analysis of GATA3 expression was performed as described previously (44).

Retroviral vectors and infection

cDNA for human GATA3 was inserted into a multicloning site of pMX-IRES-GFP (16). The methods for the generation of the virus supernatant and infection were described previously (16).

OVA immunization and ELISA for the measurement of serum Ig concentration

Young (6 wk old) and old (10 mo old) BALB/c mice were immunized i.p. with 100 μg of OVA emulsified in CFA (Difco) on days 0 and 7. Blood was collected from the tail vain on day 14. The concentrations of IgE in the serum were measured with a mouse IgE ELISA kit (BD Biosciences). The concentrations of OVA-specific Igs (IgG1 and IgG2a) in the serum were determined by ELISA as described previously (5).

Immunoblotting

Immunoblotting was performed as described previously (6). For ERK1 and ERK2 phosphorylation, naive $CD4^+$ T cells from C57BL/6 mice were purified with anti-CD4 mAb (RM4-5) and magnetic beads sorting (MACS sorting), and then the cells were incubated with anti-TCR mAb (H57-597) on ice. After incubation, the cells were stimulated with anti-hamster Igs (which cross-reacts with both H57-597) for 3, 10, or 30 min at 37°C, and then total cell lysates were subjected to phospho-ERK immunoblotting (Cell Signaling Technology). For STAT6 phosphorylation, naive $CD4^+$ T cells from C57BL/6 mice were activated with immobilized anti-TCR mAb and IL-4 (100 U/ml) for 2 days (induction culture). To assess IL-4-induced tyrosine phosphorylation, stimulated cells were washed, cultured for 8 h without cytokines, and stimulated with IL-4 (100 U/ml) for 3, 10, 30, or 60 min at 37°C. For IL-4 titration, 10–100 U/ml IL-4 was used. Anti-phosphotyrosine (RC20; BD Transduction Laboratories) or antiserum reactive with STAT6 (R&D Systems) was used for detection. For the detection of GATA3 or JunB, nuclear extracts were prepared with NE-PER Nuclear and Cytoplasmic Extraction Reagent (Pierce) according to the manufacturer's protocol. Immunoblotting was performed with anti-GATA3 mAb or anti-JunB mAb (Santa Cruz Biotechnology). HRP-conjugated anti-mouse Ig Ab (Amersham Biosciences) was used for GATA3 or JunB visualization (45).

Chromatin immunoprecipitation (ChIP) assay

Acetylation status of histone H3-K9/K4 was assessed using histone H3 (K9/14) ChIP assay kits (no. 17-245; Upstate Biotechnology) as described previously (46). The ChIP assay for di-methylated histone H3-K4 was performed using anti-histone H3 dimethyl K4 antiserum (no. 07-030; Upstate Biotechnology) (47). Semiquantitative PCR was performed with DNA samples from 3×10^4 or 1×10^4 cells at 28 cycles. PCR products were resolved in an agarose gel and visualized and quantified using an ATTO L&S analyzer (ATTO). The primers used were described previously (46).

Sensitization and inhalation with OVA

Young (6 wk old) and old (12 mo old) BALB/c mice were immunized i.p. with 250 μg of OVA (chicken egg albumin purchased from Sigma-Aldrich) in 4 mg of aluminum hydroxide gel (alum) on days 0 and 7. Mice were made to inhale aerosolized OVA in saline (10 mg/ml) for 30 min. using a supersonic nebulizer (model NE-U07; Omron) on days 14 and 16 to assess eosinophilic inflammation as described previously (48).

Collection of bronchioalveolar lavage (BAL) fluid and lung histology

Two days after the last OVA inhalation on day 16, BAL was performed as described previously (49). Total BAL fluid was collected and the cells in 100-μl aliquots were counted. One hundred thousand viable BAL cells were cytocentrifuged onto slides using a Cytospin3 (Thermo Shandon) and stained with May-Grüenwald-Giemsa solution (Merck) as described previously (50). Two hundred leukocytes were counted on each slide. Cell types were identified using morphological criteria. The percentages of each cell type were calculated.

For lung histology, mice were sacrificed by CO_2 asphyxiation 48 h after the last OVA inhalation on day 16, and the lungs were infused with 10% (v/v) Formalin in PBS for fixation. The lung samples were sectioned, stained with H&E reagents, and examined for pathological changes under a light microscope at ×200. Numbers of infiltrated mononuclear cells in the perivascular and peribronchiolar regions were enumerated by direct counting of four different fields per slide as described previously (51).

Results

Phenotypic and functional characterization of aging mouse CD4$^+$ T cells

We initiated the analysis of T cells of aging C57BL/6 mice (8–12 mo) maintained under specific pathogen-free conditions by examining the expression of cell surface molecules on splenic CD4$^+$ T cells. Representative CD4/CD8 profiles for young and aging mice are shown in Fig. 1*A*. The yields of spleen cells were 112 ± 24 × 10^6 (n = 8) for young mice and 134 ± 34 × 10^6 (n = 8) for aging mice. The percentages of CD4$^+$ and CD8$^+$ T cells in the spleen were similar between young and aging mice, and the cell surface expression of TCR$\alpha\beta$ and CD3 on the splenic CD4$^+$ T cells was also similar (Fig. 1*B*). However, the numbers of CD25$^+$ cells, CD69$^+$ cells, and memory type (CD44^{high}) CD4$^+$ T cells in aging mice were higher than in young mice. The expression level of IL-4Rα on CD4$^+$ T cells was slightly higher in aging mice. As for T cell function, the anti-TCRβ mAb-induced proliferative responses of CD4$^+$ T cells were lower in aging mice (Fig. 1*C*). We examined the anti-TCR-induced cell division of CD4$^+$ T cells in Th1- or Th2-skewed differentiation cultures and found that CFSE-labeled naive CD4$^+$ T cells were stimulated by the anti-TCRβ mAb in the presence of IL-2 and IL-12 (Th1 culture conditions) or IL-2 and IL-4 (Th2 culture conditions). After 72 h of culture, the cells had divided three to four times in the case of both young and aging mouse T cells. The rate of cell division of aging mouse CD4$^+$ T cells was slightly impaired under either Th1- or Th2-skewed conditions (Fig. 1*D*). Similar results were obtained using CD4$^+$ T cells form BALB/c mice (data not shown). These results suggest that CD4$^+$ T cells from aging mice have a moderately decreased proliferative response to anti-TCR stimulation, a finding consistent with previous reports (17, 18).

In vitro Th1/Th2 cell differentiation of naive CD4$^+$ T cells from aging mice

Th1/Th2 cell differentiation of naive CD4$^+$ T cells from young and aging mice was examined using a well-established in vitro culture system (5). Naive CD4$^+$ T cells from aging OVA-specific TCR$\alpha\beta$ Tg (DO11.10 Tg) mice were sorted and stimulated with antigenic OVA peptide in the presence of young BALB/c APCs for 5 days. CD4$^+$ T cells from young DO11.10 Tg mice preferentially differentiated into IL-4-producing Th2 cells in an Ag dose-dependent fashion (Fig. 2, *left upper panels*). However, for aging mice, the generation of Th2 cells was decreased, and a significant increase in the number of IFN-γ-producing Th1 T cells was observed (Fig. 2, *left panels*). The levels of Th2 cell differentiation induced by a minimal dose of antigenic peptide (0.1 μM), and exogenous IL-4 was also decreased in old DO11.10 Tg T cell cultures (Fig. 2, *middle panels*). In contrast, the IL-12-dependent induction of Th1 cell differentiation remained intact (Fig. 2, *right panels*). These results suggest that the efficiency of Th2 cell differentiation is reduced in aging mice.

Anti-TCR-induced cytokine production profiles of splenic CD4$^+$ T cells from aging mice

Purified BALB/c CD4$^+$ T cells from young and aging mice were stimulated in vitro with immobilized anti-TCRβ mAb, and the level of cytokines in the culture supernatant was determined by ELISA (Fig. 3). The levels of IL-2 were not obviously decreased on day 2 but decreased on day 3. The production of IFN-γ in aging mouse CD4$^+$ T cell cultures was substantially increased on day 5 and day 7. In contrast, the levels of all Th2 cytokines, IL-4, IL-5, and IL-13, in aging mouse T cell cultures were decreased on days

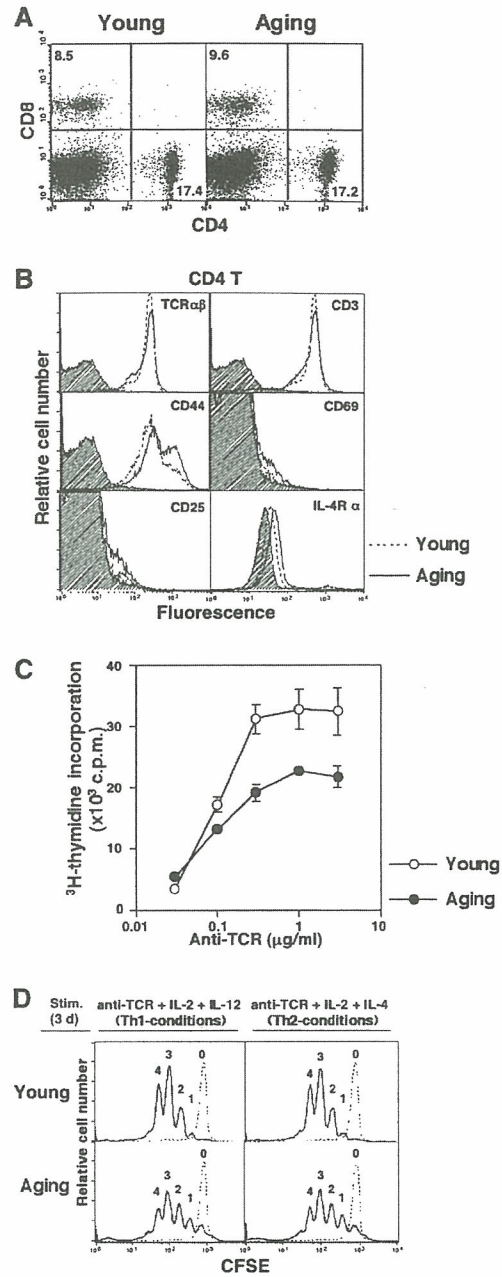

FIGURE 1. Phenotypic and functional characterization of aging mouse T cells. *A*, Representative CD4/CD8 profiles of splenocytes of young (6 wk old) and aging (9 mo old) C57BL/6 mice are shown. Percentages of cells present in each area are also shown. *B*, Each histogram depicts the expression of the indicated marker Ags on electronically gated splenic CD4$^+$ T cells from young (dotted lines) and aging (solid lines) mice. Background staining is shown as hatched areas. *C*, Splenic CD4$^+$ T cells from young (○) and aging (●) mice were stimulated with immobilized anti-TCRβ mAb. The mean [^{3}H]thymidine incorporation of each group is shown with SDs. *D*, Naive CD4$^+$ T cells were labeled with CFSE and stimulated with immobilized anti-TCRβ mAb under Th1- or Th2-skewed conditions. After 3 days of culture, the number of cell divisions (0 to 4) was assessed by flow cytometry.

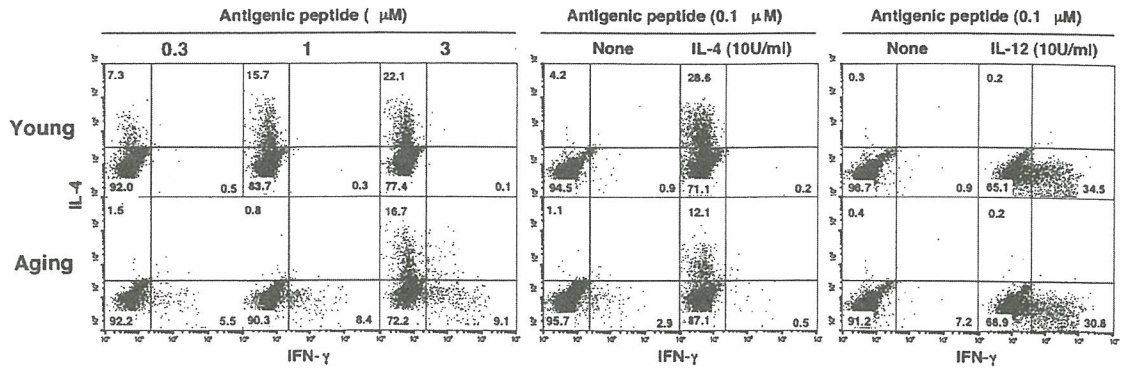

FIGURE 2. In vitro Th1/Th2 cell differentiation of naive CD4$^+$ T cells from aging mice. Naive (CD44^{low}) CD4$^+$ T cells purified by cell sorting from the spleens of aging OVA-specific TCR$\alpha\beta$ Tg (DO11.10 Tg) mice were stimulated with the indicated doses of antigenic peptide (OVA; 323–339) and irradiated young BALB/c APCs (*left panel*), a minimal dose of peptide (0.1 μM) and APCs in the presence of exogenous IL-4 (*middle panel*) or IL-12 and anti-IL-4 mAb (*right panel*) for 5 days. Intracellular staining profiles of IFN-γ and IL-4 are shown with percentages of cells in each area. The results are representative of five experiments.

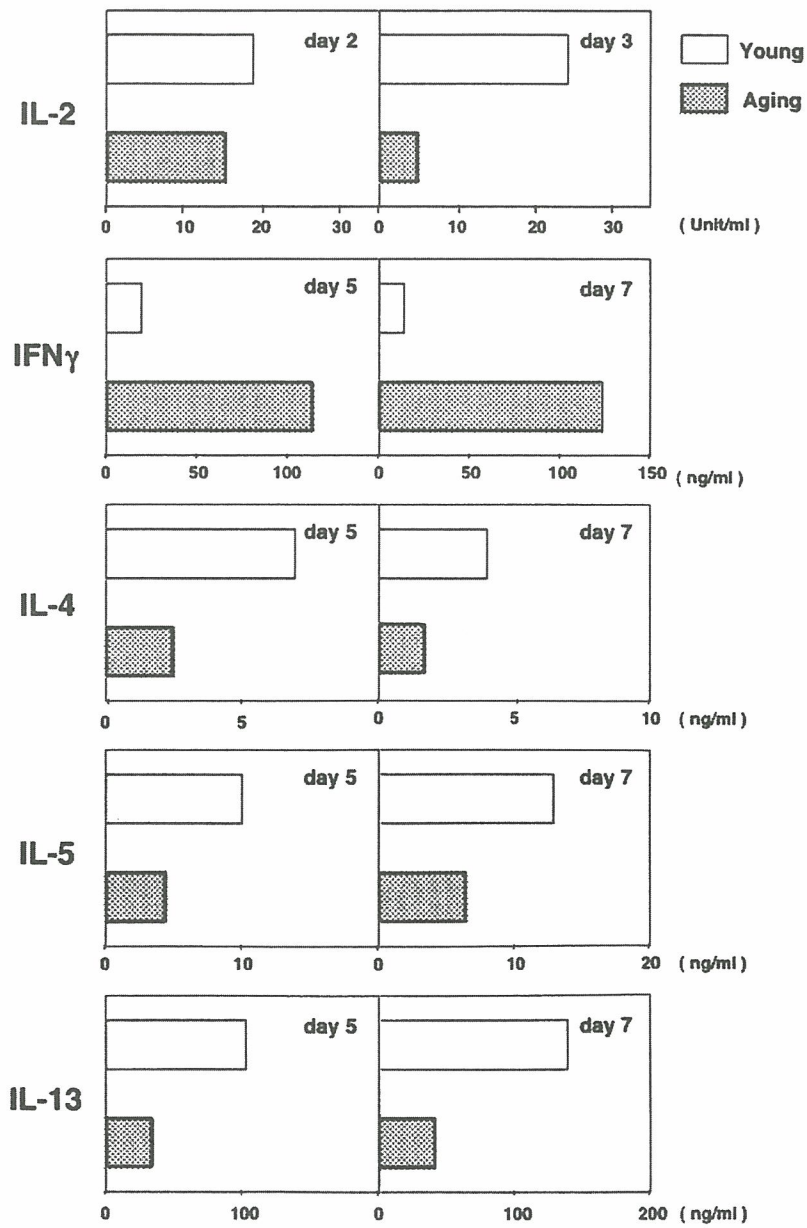

FIGURE 3. Decreased Th2 cytokine production in aging mouse CD4$^+$ T cells. Purified BALB/c splenic CD4$^+$ T cells were stimulated with immobilized anti-TCRβ mAb for 2 and 3 days (IL-2), or 5 and 7 days (IL-4, IL-5, IL-13, and IFN-γ). The concentration of cytokines in the culture supernatant was determined by ELISA. Three independent experiments were performed with similar results.